

# Advanced strategies for constructing interfacial tissues of bone and tendon/ligament

Journal of Tissue Engineering  
Volume 13: 1–31  
© The Author(s) 2022  
Article reuse guidelines:  
sagepub.com/journals-permissions  
DOI: 10.1177/20417314221144714  
journals.sagepub.com/home/tej



Wangwang Luo<sup>1\*</sup>, Yang Wang<sup>1</sup>, Qing Han<sup>1\*</sup>, Zhonghan Wang<sup>1,2</sup>, Jianhang Jiao<sup>1</sup>, Xuqiang Gong<sup>1</sup>, Yang Liu<sup>1</sup>, Aobo Zhang<sup>1</sup>, Han Zhang<sup>1</sup>, Hao Chen<sup>1</sup>, Jincheng Wang<sup>1</sup> and Minfei Wu<sup>1</sup> 

## Abstract

Enthesis, the interfacial tissue between a tendon/ligament and bone, exhibits a complex histological transition from soft to hard tissue, which significantly complicates its repair and regeneration after injury. Because traditional surgical treatments for enthesitis injury are not satisfactory, tissue engineering has emerged as a strategy for improving treatment success. Rapid advances in enthesitis tissue engineering have led to the development of several strategies for promoting enthesitis tissue regeneration, including biological scaffolds, cells, growth factors, and biophysical modulation. In this review, we discuss recent advances in enthesitis tissue engineering, particularly the use of biological scaffolds, as well as perspectives on the future directions in enthesitis tissue engineering.

## Keywords

Enthesis, tendon, ligament, tissue engineering

Date received: 28 July 2022; accepted: 26 November 2022

## Introduction

Enthesis is a key component of the tendon and ligament that forms a bridge between soft and hard tissues (tendon/ligament and bone) through the fibrous, unmineralized fibrocartilagenous, mineralized fibrocartilagenous, and bony regions.<sup>1,2</sup> Enthesis also supports the mechanical transmission of tensile stress and force from the main body of the tendon/ligament to the bone surface.<sup>3–5</sup> Because of its location between the tendon/ligament and the bone, the enthesitis is frequently damaged during avulsion fracture and ankylosing spondylitis.<sup>6,7</sup> The incidence rate of enthesitis orthopedic injury has increased markedly in recent years, and each year, around 30 million people undergo enthesitis reconstruction in the United States and Europe, which costs over 163 billion dollars.<sup>8,9</sup> For example, in the USA, it is estimated that >100,000 reconstructions are done for anterior cruciate ligament (ACL) enthesitis each year at a cost of >1.5 billion dollars.<sup>10</sup> Thus, effective strategies for regenerating injured enthesitis are urgently needed.

Traditional surgical treatments for enthesitis include the reconstruction of enthesitis with broken tendon/ligament

terminals.<sup>11–13</sup> This is achieved through: (a) direct insertion of the broken enthesitis into the bone tunnel, (b) mechanical anchoring of the reconstructed tissue using sutures or screws, and (c) minimizing externally-loaded forces to avoid accidental loosening or re-rupture after surgery.<sup>14–19</sup>

<sup>1</sup>Department of Orthopedics, The Second Hospital of Jilin University, Changchun, China

<sup>2</sup>Orthopaedic Research Institute of Jilin Province, Changchun, China

\*These authors contributed equally to this work and are considered to be co-first authors.

### Corresponding authors:

Hao Chen, Department of Orthopedics, The Second Hospital of Jilin University, 218 Ziqiang Street, Changchun 130000, China.  
Email: chen hao7014@outlook.com

Minfei Wu, Department of Orthopedics, The Second Hospital of Jilin University, 218 Ziqiang Street, Changchun 130041, China.  
Email: wumf@jlu.edu.cn

Jincheng Wang, Department of Orthopedics, The Second Hospital of Jilin University, 218 Ziqiang Street, Changchun, China.  
Email: jinchengwangjlu@163.com



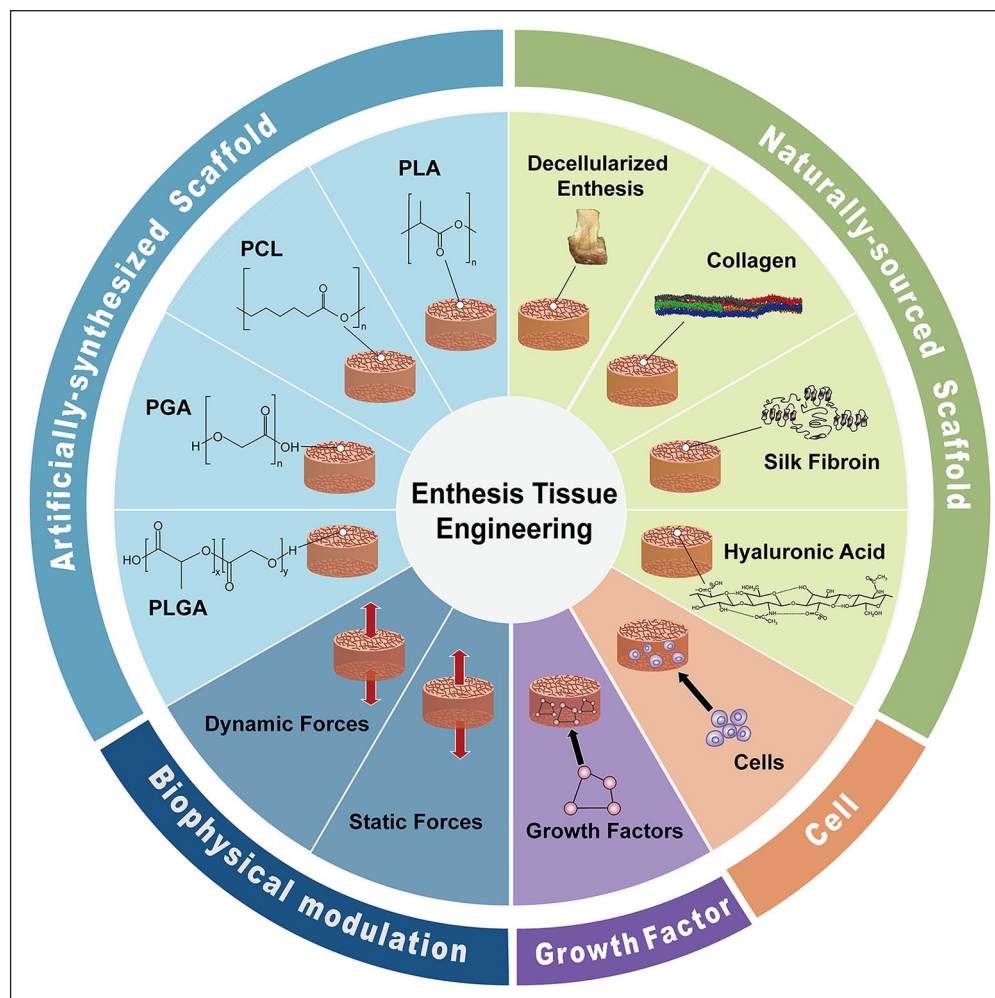


**Figure 1.** The common strategies in entheses tissue engineering.

Because traditional surgical treatments mainly focus on reestablishing entheses anatomy while overlooking entheses tissue regeneration, their efficacy in entheses repair is limited. For instance, the reestablished entheses may remain weakly connected to the bone for an extended time, leading to the formation of scar tissue instead of the desired healthy entheses tissue, and in severe cases degeneration and lysis may occur, resulting in the loss of the anatomical reconnection between the entheses and the bone.<sup>20–23</sup> Currently, the lack of effective methods of regenerating native entheses but not the weak scar tissue is a major clinical challenge, and in recent decades, entheses tissue engineering has emerged as a way of overcoming these limitations in the traditional surgical treatments.<sup>24,25</sup>

Entheses tissue engineering has led to the development of several novel methods of improving entheses regeneration. The advanced methods that are currently used in entheses tissue engineering can be divided into the biological scaffold strategy, the cell strategy, the growth factor strategy, and the biophysical modulation strategy (Figure 1).<sup>3,26–28</sup> These strategies can be used alone or in

combination to promote entheses regeneration. The biggest challenge in entheses regeneration is the lack of effective ways of generating the typical four-layered histological structure at the interface between the bone and the broken entheses tissue.<sup>24</sup> The biological scaffold strategy focuses on producing biocompatible entheses scaffolds using various biomaterials and fabrication techniques to mimic the native structure of entheses tissue as closely as possible.<sup>29–31</sup> The use of biomimetic entheses scaffolds also seeks to provide a favorable environment for entheses tissue regeneration and to offer an extra platform for the growth and infiltration of regenerative entheses tissue. To ensure that the entheses scaffold is highly biomimetic, a multilayered entheses scaffold fabricated using an elaborate design on the inner structure is required.<sup>32</sup> The cell strategy of entheses tissue engineering relies on entheses-associated cells to promote regeneration at the site of injury.<sup>26,33</sup> The growth factor and biophysical modulation strategies have been found to markedly promote entheses regeneration.<sup>34,35</sup> Mounting evidence indicates that compared with traditional surgical treatments, these entheses tissue engineering

strategies can improve regeneration of the immature four-layered enthesis tissue *in situ* at a markedly accelerated rate.<sup>36,37</sup> For example, the use of a co-electrospinning PCL nanoscaffold and collagen for the reconstruction of rat enthesis, has been shown to successfully lead to the formation of fibrocartilage tissue and the regeneration of an enthesis-like structure at the scaffold–bone interface 8 weeks after operation.<sup>38</sup> Another study reported significantly accelerated regeneration of the rotator cuff tendon enthesis after using a chemotactic decellularized fibrocartilaginous matrix graft.<sup>39</sup>

In this review, we first describe the characteristics of enthesis tissue, followed by a detailed discussion of the four strategies of enthesis tissue engineering, their practical applications, and their effects on enthesis regeneration. In the final part of the review, we discuss the current state and future research perspectives on enthesis tissue engineering.

## Characteristics of enthesis tissue

Enthesis tissue usually refers to the tendon/ligament–bone interface and not the muscle–tendon enthesis tissue. Tendons and ligaments are highly similar tissues and with the exception of the main bodies, their bony terminals—enthesis tissue—are almost identical.<sup>40–42</sup> Studies have also shown that injuries occurred in enthesis tissue are common enough.<sup>43–45</sup> In this section, we try to introduce the background information on enthesis tissue and to highlight its complex histological compositions and the natural healing process of enthesis tissue in detail.

### Enthesis tissue structure

Based on closeness to the bone surface, enthesis tissue is divided into the fibrous region (Zone I), unmineralized fibrocartilagenous region (Zone II), mineralized fibrocartilagenous region (Zone III), and bony region (Zone IV)<sup>40,42,46</sup> (Figure 2(a)–(d)).

**The fibrous region.** The fibrous region (Zone I) is made of regular special axial–hierarchical structures<sup>47</sup> (Figure 2(e)). Its basic structural unit is collagen type I, which first twists in clusters of five to form microfibrils, the primary fiber bundles. Next, large microfibril bundles spatially repeat along the axis and in parallel, forming the second fiber bundle, fibril. The fibril has a diameter of 100–500 nm, depending on the number of microfibrils it contains. However, based on electron microscopic examination, all fibrils have a biomolecular structure with the same periodicity (the D-band) irrespective of diameter. The D-band spatially recurs every 67 nm along the fibril and it dose can indicate how regularly microfibrils are distributed and combined.<sup>48</sup> Next, through the action of various biomolecules, including proteoglycans, many fibrils are crosslinked and wrapped by the primary endotenon, forming a collagen

fiber. Collagen fibers are then encapsulated by a second endotenon and an epitenon, forming a fascicle that completes the Zone I structure.<sup>49,50</sup> Both the collagen fiber and fascicle possess inner activity because the membrane and sheath that wraps them are in free contact with each other, which allows the collagen fibers and fascicles to slightly move and glide transversally.<sup>47–51</sup> With regard to histological nutrient exchange in Zone I, the vascular networks, together with some tiny nerves and lymphatic capillaries, are mainly distributed in the external layer (epitenon) and the second endotenon, and is rarely observed in the central region.<sup>50–52</sup> These microvessels have a small average diameter and blood flow through them is very slow. This indicates that total blood volume in the enthesis is much lower than in other tissues like the skin and muscles, and that the nutrient/waste–product exchange in the inner region of enthesis tissue mainly depends on diffusion through the matrices, which is not sufficient for cellular metabolic needs. This nutrient shortage may be severer during accelerated cell growth, reproduction, or differentiation. Thus, the limited nutrient exchange caused by its anatomical features can explain why the enthesis has low cellular density, with 55%–70% of the enthesis being extracellular matrix (ECM), which mainly contains water.<sup>53</sup> This may also explain why enthesis tissue healing is slow after injury.

With regard to cellular composition, Zone I is made of several cell types, including fibrocytes, fibroblasts, vascular endothelial cells, nerve cells, and various immune cells, including mast cells, neutrophils, and macrophages).<sup>54</sup> Fibrocytes are the most common cell type in Zone I, accounting for 90%–95% of all cells.<sup>53</sup> Fibrocytes are mostly derived from fibroblasts, which are locally embedded in intra-fibril spaces and have a larger variation potential and a higher reproduction rate than fibrocytes.<sup>49,55–57</sup> Fibrocytes and fibroblasts are the main producers of the ECM in Zone I and they produce almost all ECM components. Without considering water, the ECM of Zone I is mainly made of collagen fibrils, which make 60%–85% of the dry weight. Collagen type I makes up most (80%–90%) of the total collagen content, followed by collagen type III (1%–10%) and collagen type II (2%). The ECM of Zone I also contains a small amount of elastin, proteoglycans, glycosaminoglycans (GAGs), and glycoproteins. These functional biomolecules can enhance the biomechanical properties of Zone I, such as its stiffness, toughness, and viscoelasticity.<sup>49,58</sup> In enthesis tissue engineering, the factors influencing fibrogenesis might mainly function in Zone I.

**The unmineralized fibrocartilagenous region.** The unmineralized fibrocartilagenous region (Zone II) is characterized by an acute change in tissue composition, with the ECM components changing into collagen type II and III, which in humans, are typical components of the hyaline cartilage.<sup>59</sup> Zone II also contains small amounts of collagen

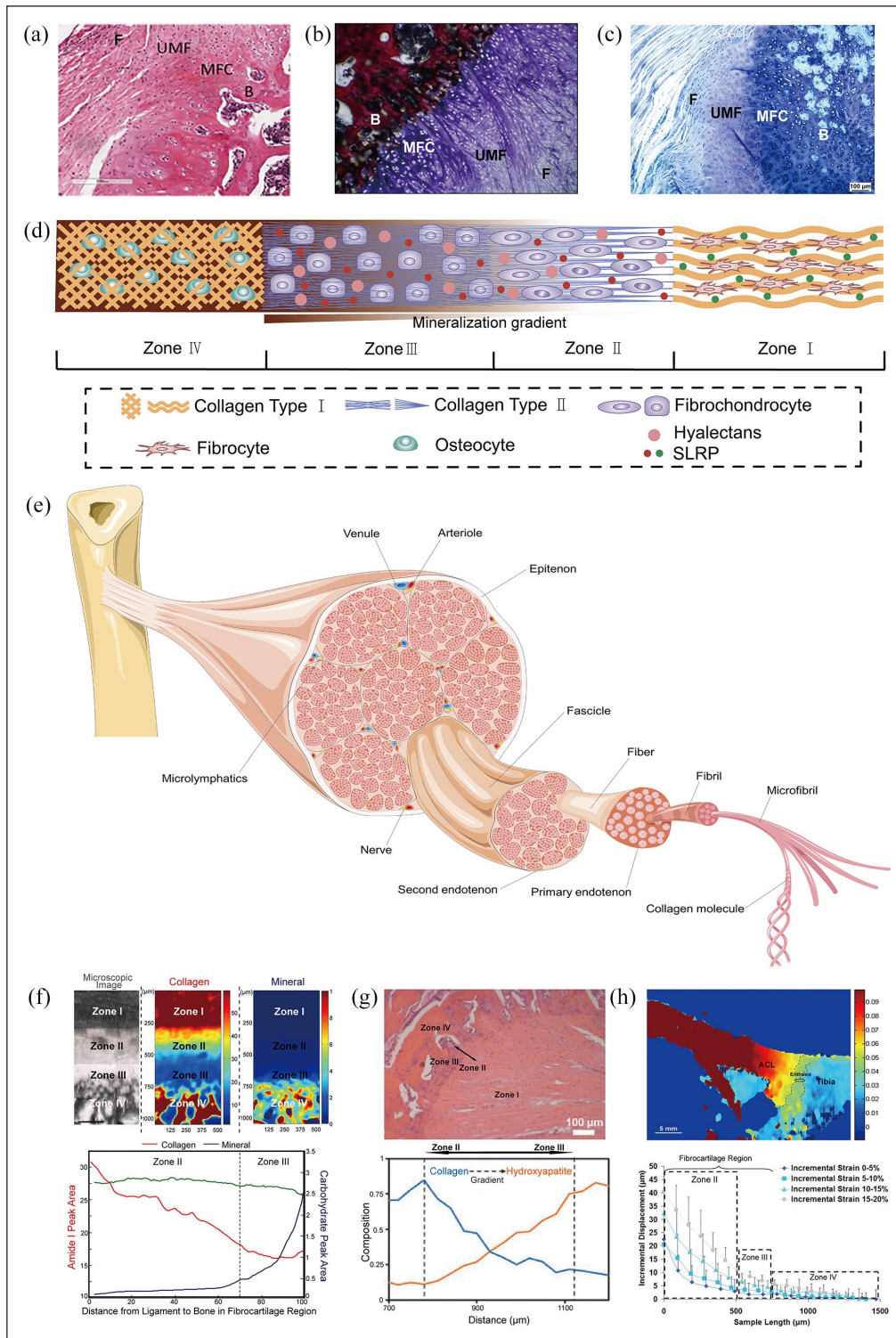


**Figure 2.** (a) Hematoxylin & Eosin image of the structure of rat enthesis,<sup>40</sup> (b) Sanderson staining and Van Gieson staining image of the structure of sheep enthesis,<sup>42</sup> (c) Giemsa staining image of the structure of sheep enthesis.<sup>46</sup> (d) A schematic representation of transition across the four zones. (e) The special axial hierarchical structure of Zone I. (f) The upper three figures are a microscopic image, a collagen distribution map under FTIR-I, and a mineral distribution map under FTIR-I in tibial ACL enthesis. The lower figure is a quantitative analysis of the collagen and mineral distribution in the enthesis fibrocartilage region.<sup>74</sup> (g) Raman spectral mapping of the gradient transition of collagen and mineral content in the fibrocartilage region of an ACL enthesis.<sup>75</sup> (h) Upper figure: an elastographic analysis of ACL enthesis in tension shows the distribution of mechanical stress experienced through the enthesis (yellow–green–blue).<sup>78</sup> Lower figure: strain response curve of an ACL enthesis under uniaxial compression.<sup>79</sup> F: fibrous region; UMF: unmineralized fibrocartilagenous region; MFC: mineralized fibrocartilagenous region; B: bony region; ACL: anterior cruciate ligament; FTIR-I: fourier transform infrared spectroscopic imaging.

type I and X, GAGs, and proteoglycans.<sup>60–63</sup> The proteoglycans in Zone II are mostly aggrecan and versican, which are large chondroitin sulfate proteoglycans (hyalectans).<sup>62–64</sup> With the exception of hyalectans, some small leucine-rich repeat proteoglycans (SLRP), such as chondroadherin and biglycan, are highly abundant in Zone II than in Zone I.<sup>65,66</sup> Hyalectans and SLRP, which occur on the surface of fibrils, are both negatively charged proteoglycans located in the gaps of collagen type II fibrils.<sup>65,67</sup> The molecular and electrostatic repulsive forces between proteoglycans and collagen fibrils cause collagen type II fibrils to diverge. The alignment of the collagen fibrils becomes slightly unparallel and irregular, and the fibrils can slide along each other, which markedly increases the degree of anisotropy.<sup>68</sup> These biomolecular features illustrate why enthesis tissue endure tensile or compressive mechanical forces in all directions. Moreover, fibrochondrocytes in Zone II are substituted for fibrocytes, which become the main cell type. However, the morphology of fibrochondrocytes is highly similar to that of fibrocytes, which are spindle-like or flat and stretched along the enthesis axis.<sup>69</sup>

**The mineralized fibrocartilagenous region.** Zone II and the mineralized fibrocartilagenous region (Zone III) are both fibrocartilagenous tissues but differ in their degree of tissue calcification. In Zone III, collagen type X is the second most abundant component of collagen fibrils instead of collagen type III, and collagen type II is still predominant although its overall fibril alignment is more random and anisotropic, which may be caused by increased levels of aggrecan and versican.<sup>59,62,63</sup> Although tissue mineralization starts to appear in this region, it is incomplete. The mineral in this area is amorphous calcium phosphate (ACP), which does not directly interact with collagen molecules but can interact with other structural biomolecules like proteoglycans, GAGs, and glycoproteins via their charged amino acid residues, particularly the negatively charged residues on carboxyl groups.<sup>70,71</sup> Because of the low amount of non-collagenous protein and their binding capability with ACP, the mineralization process in Zone III is interrupted in the early stage. This may be why no crystalline calcium phosphate can be formed ulteriorly.<sup>72</sup> In Zone III, the cells are predominantly fibrochondrocytes with different morphologies and distributions. Fibrochondrocytes have a larger volume and rounder shape and are stochastically distributed in the network of collagen fibrils.<sup>69</sup> In enthesis tissue engineering, strategies for promoting chondrogenesis usually target both Zone II and III.

**Bony region.** The bony region (Zone IV) has the maximum level of histological mineralization. The predominant collagen fibrils, mineralized by hydroxyapatite, revert to collagen type I while osteocytes, osteoblasts, and osteoclasts, become randomly scattered in the bony ECM network.<sup>73</sup> In enthesis engineering, the enhancement of osteogenesis

via various strategies can vastly improve Zone IV regeneration.

**The structure transition from Zone I to Zone IV.** It is clear that progression from Zone I to Zone IV is accompanied by an abrupt change from soft to hard tissue. In enthesis tissue, structural transition is compositionally distinct and graded in the interfaces between Zone I and II as well as Zone III and Zone IV, while at the same time, there is also a continuous structural gradient from Zone II to Zone III (Figure 2(f)).<sup>74,75</sup> In the Zone II–Zone III span, hydroxyapatite levels increase continuously but relatively more rapidly in Zone III, whereas collagen levels decrease gradually, indicating the existence of a gradient transition between the two fibrocartilagenous zones (Figure 2(g)).<sup>75</sup> With regard to the structure–function relationship in the four zones, the typical multi-layered tissue transition and its spatial heterogeneity closely correlate with the distribution of the mechanical stress experienced through the enthesis.<sup>76–79</sup> An elastographic analysis of tension-loaded ACL enthesis found that the highest displacement was in Zone I and that the peak value decreased gradedly from Zone I to Zone II, gradiently from Zone II to Zone III, and gradedly from Zone III to Zone IV, indicating an overall increase in tissue stiffness that corresponded with structural transition through the four zones (Figure 2(h)).<sup>78</sup> Moreover, an analysis of region-dependent strain response by the ACL enthesis under uniaxial unconfined compression found that incremental displacement decreased continuously from Zone II to Zone III, which may indicate that increasing tissue stiffness corresponds to structural transition in these two zones (Figure 2(h)).<sup>79</sup> Taken together, the characteristics of enthesis tissue discussed above are key in minimizing stress concentration and promoting gradual load transfer from the soft to hard tissue. These characteristics might also explain why this small soft–hard region (within a few hundreds of micrometers) endure relatively high local tensile/compressive stresses and forces without failure, deformation, or tear.

### *The natural healing process of enthesis*

The natural healing process of enthesis is complex and can be divided into three phases: a) the inflammatory and necrotic phase (early period), b) the rapid proliferative phase (middle period), c) the gradual remodeling phase (final period).<sup>80–82</sup> The inflammatory and necrotic phases usually occur in the first week of injury. Inflammation is triggered by inflammatory factors that target fibroblasts, fibrocytes, and vascular endothelial cells, resulting in cytotoxicity of the damaged tissue.<sup>83–89</sup> During this period, the biological structure and biomechanical properties of the injured enthesis deteriorate rapidly, severely limiting regeneration capacity. Therefore, suppressing inflammation in the early period is crucial for good recovery.<sup>90,91</sup> Because the levels of the inflammatory mediators interleukin

**Table 1.** The biological scaffolds, cells, growth factors, and biophysical modulations applied in entheses tissue engineering.

Biological scaffolds		Cells	Growth Factors	Biophysical Modulations
Natural Scaffolds	Artificial Scaffolds			
Decellularized entheses	Polyolefins	Osteoblasts	BMPs	Stress stimulation
Collagen	Poly(urethanes)	Fibroblasts	FGFs	Electromagnetic field
Silk	PLA	CDSCs	TGFs	
HA	PCL	TSPCs	GDFs	
	PGA	ADSCs	PDGFs	
	PLGA	MSCs	VEGF	

(IL)-1 $\beta$ , IL-6, IL-8, tumor necrosis factor (TNF), matrix metalloproteinase (MMP)-1, MMP-3, and MMP-13 are upregulated in the early period of entheses healing,<sup>92,93</sup> there are several potential targets for effectively inhibiting inflammatory reactions. After inflammation subsides, the injured entheses enters the rapid proliferation phase, which usually lasts from the first to the third or fourth week of injury and leads to marked increases in the number of nearly all cell lineages in the entheses, including fibrocytes, fibroblasts, fibrochondrocytes, osteocytes, and vascular endothelial cells. The production and secretion of the ECM, which is mainly made of collagen type III, also accelerates.<sup>94</sup> This results in new entheses tissue although at this stage it is immature and fragile, and its biomechanical properties have not met healing requirements. The last phase of healing is the long remodeling period which typically lasts several months or years. This process is characterized by a significant decrease in the total cellular density and a continuous increase in the number of fibroblasts, decrease in ECM content and overall production of collagen and GAGs, and a gradual increase in the production of collagen type I.<sup>95,96</sup> In this period the typical four-layer physiological structure of the entheses slowly rebuilds and the maximum stress loading capacity rises.<sup>97–99</sup> However, after natural recovery, the entheses tissue is far weaker than the uninjured tissue. Perfect natural healing is not achievable and there is risk that the regenerated entheses tissue may re-rupture and undergo resorption.<sup>94,95</sup> Moreover, entheses healing is nonuniform and intrinsic healing process is relatively slower than extrinsic healing, probably because of the heterogeneity of the vascular network distribution in entheses tissue.<sup>100–102</sup>

Based on the natural characteristics of entheses tissue listed above, numerous recent studies have attempted to promote entheses regeneration and identified several factors that may effectively improve entheses regeneration, including bio-gels, scaffolds, growth factors, and stem cells.<sup>103–107</sup>

## Tissue engineering strategies for entheses reconstruction

The field of tissue engineering (TE) involves several disciplines, such as cytology, histology, molecular biology, biochemistry, material science, engineering science, and

clinical medicine. The concept of TE was first introduced in 1993 by Langer and Vacanti and its overall aim is to develop feasible methods of artificially rebuilding various tissues and organs.<sup>108,109</sup> TE, which not only seeks to reconstruct histological structures, but also to restore original biological functions, has been widely applied in orthopedics and there are several strategies for repairing bone defects.<sup>110–112</sup> However, the development of entheses TE is not as advanced and the successful reconstruction of entheses tissue has not yet been achieved.<sup>3,26,113–115</sup> Studies on the use of TE in entheses repair involve four strategies, the biological scaffold, cell, growth factor, and biophysical modulation strategies. Of these, the biological scaffold strategy has attracted the most interest (Table 1).

### The biological scaffold strategy

A suitable biological entheses scaffold should have the following properties: (a) a biomimetic structure, (b) mechanically biomimetic properties, (c) mouldability, (d) biodegradability, and (e) biocompatibility (should not be cytotoxic or inflammatory).<sup>3,42,116–118</sup> These requirements markedly limit the number of materials that can be used as biological scaffolds in entheses TE. Entheses scaffolds can be natural or artificial.<sup>119–127</sup> Artificial entheses scaffolds are fabricated using synthetic polymeric biomaterials, whereas natural ones are made of natural materials like collagen, silk fibroin, and hyaluronic acid. The most straightforward approach for developing entheses biological scaffolds involves decellularized entheses tissue from laboratory animals or human donors. In the following sections we discuss the common types of scaffolds in detail.

**Decellularized scaffolds.** Decellularized entheses scaffolds, which are the most readily available, fall into three categories based on their origin—autogenous entheses scaffolds, allogeneic entheses scaffolds, and xenogeneic entheses scaffolds.<sup>128,129</sup> Although their tissue sources are different, the principle of scaffold-making is largely the same and involves depletion of the cellular component of raw entheses tissue to obtain the ECM only, which can form a entheses biological scaffold.<sup>130</sup> The main advantage of decellularized entheses scaffolds are that they are easy to obtain and the tissue's biomimetic capacity is

guaranteed (especially when the scaffold is based on the same anatomical site).<sup>131,132</sup>

A study by Xu et al. which developed a porcine decellularized Achilles enthesis scaffold using a new protocol, found that the decellularized enthesis scaffold preserved the typical histological structure of enthesis tissue well (Figure 3(a)).<sup>133</sup> Additionally, their biomechanical assessment showed that the decellularized enthesis scaffold retained mechanical properties that were appropriate for practical applications (Figure 3(b)).<sup>133</sup> A study by Su et al. produced a porcine decellularized Achilles enthesis scaffold using a refined protocol and found that it promotes enthesis regeneration in vitro and in vivo (Figure 3(c)).<sup>134</sup> Compared with the control group (a simple decellularized tendon scaffold), more mesenchymal stem cells (MSCs) adhered, proliferated, and infiltrated the decellularized enthesis scaffold (Figure 3(d)). The MSCs in this scaffold significantly upregulated osteogenesis-associated genes like RUNX2, OPN, and ALP, as well as tenogenesis-associated genes like SCX, THBS4, and VIM (Figure 3(e)), and when implanted into rabbit tibia, the enthesis scaffold induced the regrowth of enthesis tissue (Figure 3(f)).<sup>134</sup>

These experiments indicate that decellularized enthesis scaffolds have enormous potential for use in enthesis TE. However, decellularized scaffolds have limitations. Although the harvest of raw enthesis tissue is not difficult, decellularization and manufacturing protocols should be improved to increase efficiency.<sup>134</sup> The cellular component of raw enthesis tissue still cannot be removed radically and the structural and biomechanical properties of the enthesis's ECM may be disrupted during decellularization.<sup>133,135</sup> To improve enthesis scaffold decellularization, Shi et al. developed a vacuum aspiration system (VAS), which provides a negative pressure environment that maintains a continuous flow of phosphate buffered saline. Their experiments showed that the VAS considerably improves ECM preservation while minimizing the amount of remnant cells in the decellularized enthesis scaffold. Compared with traditionally-decellularized scaffolds, the mechanical properties of their optimized decellularized scaffold were significantly improved. Moreover, VAS-mediated scaffold decellularization effectively enhanced enthesis regeneration and osteogenic, chondrogenic, and tenogenic differentiation capacities were all elevated in the corresponding zones of this scaffold.<sup>136</sup> Therefore, VAS may significantly improve the production of decellularized enthesis scaffolds. Another key shortcoming of decellularized enthesis scaffolds is that scaffold size and its inner structure are uncontrollable and fixed individually in the different scaffolds. Currently, uniform decellularized enthesis scaffolds cannot be produced and their structures are hard to modulate.

**Collagen scaffolds.** Biomaterials based on collagen, the main component of the enthesis ECM, are widely used in medicine because of their relatively assured biocompatibility.

Collagen biomaterials have been certified by the US Food and Drug Administration for decades and collagen scaffolds have been widely used in TE.<sup>137</sup> Collagen is easily accessible and is present several tissues types, including bone and skin.<sup>138–140</sup> In the past, collagen was extracted from bone, tendon and fascia tissues via several steps that included digestion and hydrolysis,<sup>141,142</sup> which preserved its amino acid sequence, molecular structure, and biomechanical properties, and therefore its biocompatibility. After extraction, collagen would be dissolved in a buffer solution that was then used to make collagen enthesis scaffolds using various methods.<sup>143–155</sup>

The electrospun collagen enthesis scaffold, an easily accessible scaffold fabricated using an electrospinning device, is one of the most commonly used TE scaffolds and it effectively supports enthesis regeneration.<sup>38,117</sup> Based on the poly( $\epsilon$ -caprolactone) (PCL) electrospun nanofiber membrane scaffold fabricated using a simple PCL organic solution, Lin et al. added a collagen I (COL-1) solution into PCL solution and successfully fabricated a new type of a COL-1/PCL hybrid nanofiber membrane scaffold.<sup>156</sup> Mechanical and in vitro experiments, revealed that COL-1 markedly increased the porosity, hydrophilicity, and dissolution rate of the nanofiber membrane scaffold, indicating that COL-1 may improve the cellular affinity and biodegradability of the enthesis scaffold.<sup>156</sup> Moreover, tendon stem/progenitor cells (TSPCs) seeded on this COL-1/PCL hybrid scaffold exhibited a faster proliferation rate and a more widely spread cellular morphology, and highly upregulated several osteogenic differentiation genes, including Colla1, OCN, RUNX-2, and OCT-4. Experiments in which the blending volume ratios of COL-1 and PCL solution were adjusted to fabricate different scaffolds revealed that the beneficial effects mentioned above were better in the hybrid nanofiber membrane scaffold made from a 1:2 (v/v) COL-1/PCL solution (Figure 4(a)–(d)).<sup>156</sup> Together, these findings highlight collagen as an ideal biomaterial for enthesis regeneration, and show that the electrospun collagen enthesis scaffold may simultaneously promote regeneration in Zone I and IV. Apart from electrospun collagen enthesis scaffold, freeze-dried collagen enthesis scaffold is frequently applied in enthesis tissue engineering (TE). Through tuning the collagen solution temperature, the solvent (water) is first frozen to successfully segregate the dissolved collagen and the solvent, the mixture is freeze-dried to remove the ice crystal and then a porous spongy-like collagen enthesis scaffold is generated. By adjusting the concentrations of the collagen solute or choosing different manufacturing protocols, both the inner structures and the overall mechanical properties of the collagen scaffold can be artificially controlled.<sup>157–159</sup>

Based on this freeze-frying fabricating process, Caliri et al. designed and manufactured a freeze-dried biphasic collagen and a GAG (CG)/GAG and Calcium phosphate (CGCaP) enthesis scaffold. The scanning

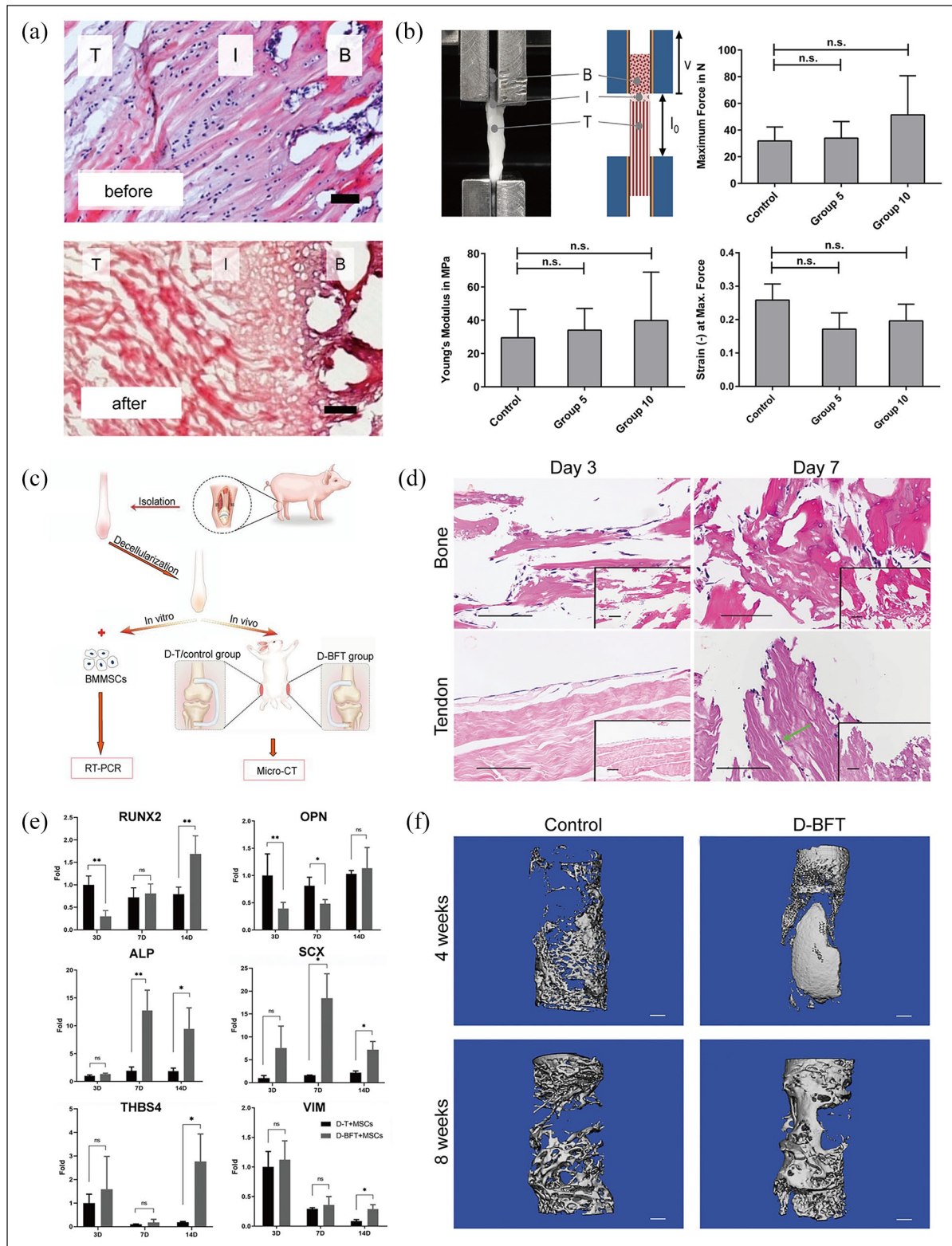


**Figure 3.** (a) Native enthesis tissue before and after decellularization,<sup>133</sup> (b) The decellularized enthesis scaffold exhibits good biomechanical properties (maximum force, Young's modulus, strain at maximum force),<sup>133</sup> (c) The process of obtaining decellularized enthesis scaffolds,<sup>134</sup> (d) Successful infiltration and proliferation of MSCs in the decellularized enthesis scaffold,<sup>134</sup> (e) Osteogenesis-associated genes (RUNX2, OPN, ALP) and tenogenesis-associated genes (SCX, THBS4, VIM) were upregulated in the decellularized enthesis scaffold, and<sup>134</sup> (f) More tissue was regenerated in the decellularized enthesis scaffold.<sup>134</sup> T: tendon; I: interface; B: bone; D-T: decellularized tendon scaffold; D-BFT: decellularized bone-fibrocartilage-tendon scaffold.



electron micrographs (SEM) of this biphasic enthesis scaffold demonstrated that the pores in the non-mineralized CG layer were longitudinally aligned and regular (corresponding to Zone I), while the pores in the mineralized CGCaP layer were relatively more isotropic and random (corresponding to Zone IV). Besides, at the interface between the two layers, the transforming collagen trabeculae were smooth and continuous (corresponding to Zone II and Zone III) (Figure 4(e)).<sup>160</sup> All the structures generated in this scaffold perfectly mimicked the native composition of the enthesis tissue. *In vitro* analysis of the scaffold showed that several fibronectin-related integrins ( $\alpha 4$ ,  $\alpha 5$ ,  $\alpha V$ ,  $\beta 1$ ,  $\beta 3$ ) and tenogenic genes (COL1A1, TNC, SCX) were highly expressed in the tendinous (CG) layer, while several osteogenic genes (BSP, ALP, OCN) were overexpressed in the osseous (CGCaP) layer.<sup>160</sup> Therefore, the freeze-dried CG/CGCaP biphasic enthesis scaffold had an excellent effect on enthesis regeneration, and could be applied in enthesis TE to promote Zone I and Zone IV regeneration in the enthesis tissue. In their follow-up studies, the researchers added a polyethylene glycol (PEG) hydrogel layer between the two layers (CG and CGCaP) to fabricate a CG-PEG-CGCaP triphasic enthesis scaffold, followed by a detailed analysis of its inner topology and mechanical properties (Figure 4(f)).<sup>161</sup> This triphasic enthesis scaffold had even more similarity with the native enthesis tissue, and thus once its biofunctions on enthesis regeneration is certified, it would possibly be another effective enthesis scaffold to be utilized in enthesis TE.

Besides the above scaffolds, the utility of electrochemical collagen enthesis scaffold in enthesis TE is also remarkable. After application of an electric field to the collagen solution, there is electrolysis of water which creates a pH gradient from the anode to the cathode. Thereafter, the dissolved collagen molecules slowly migrate and assemble at the isoelectric point (pI) region. Finally, simple collagen threads, sheets or membranes are generated, which are ulteriorly fabricated into more complex scaffolds.<sup>162–164</sup> Using this convenient fabricating process, Younesi et al. produced a plate-arcade-plate composite electrochemical collagen scaffold to emulate natural interdigitated arcade structure of the cartilage (Figure 4(g)). After seeding MSCs into the scaffold and culturing them for different periods, the studies showed that both the cell number and the scaffold weight gradually increased. H&E and Masson-trichrome staining showed that cartilage ECM slowly filled the scaffold pores with time. On the other hand, Safranin O staining demonstrated that the GAG components were produced by day 14 and were more abundant on day 28. In addition, immunostaining assay showed high generation of collagen type II and aggrecan molecules, which are the two major compositions of cartilage tissue. Moreover, Young's modulus of the cell-seeded scaffold

increased to around 60% to a cartilage-nearing value of  $1.33 \pm 0.37$  MPa. These findings demonstrated that the composite electrochemical collagen scaffold had enormous potential for cartilage regeneration, and it could be applied in enthesis TE to help regenerate the chondral parts of enthesis tissue, which correspond to the Zone II and Zone IV.<sup>165</sup>

Unlike the decellularized enthesis scaffold with a fixed collagen layout, the collagen enthesis scaffold is fundamentally fabricated with collagen molecules and its fibers in different methods, which has a higher degree of modularity of the scaffold inner architectures. Because the artificial collagen fibers possess excellent stiffness and toughness, the collagen enthesis scaffolds often have advanced mechanical properties.<sup>166</sup> Besides, since the natural collagen molecules are kept unchanged in the whole process, some cell adhesion signal targets in the collagen can be preserved, which explains why collagen scaffolds could promote cellular adhesion and proliferation as well as effective enthesis regeneration.<sup>3,117,167–169</sup> Different collagen enthesis scaffolds may target on the different regions of enthesis tissues and exert different bioeffects on enthesis regeneration. Therefore, it is feasible to hybridize these scaffolds to fabricate a more omnipotent enthesis scaffold, such as the hybridization of electrochemical collagen enthesis scaffold and electrospun collagen enthesis scaffold.

Although collagen enthesis scaffold exhibits many advantages with relatively clear functions on enthesis regeneration, collagen is mostly extracted from experimental animal tissues (rat tail or bovine Achilles tendons) or the donor's tissues.<sup>170–172</sup> Before being further processed and fabricated into scaffolds, collagen needs preconditioning to inactivate the xenoantigen or alloantigen. Collagen extracted from other animal species require mandatory preconditioning processes for biocompatibility adaptation.<sup>173,174</sup> Besides, the process of sterilization for collagen is also necessary to eliminate potential pathogens. However, it is still difficult to fully eliminate the antigens and pathogens without damaging the collagen molecules.<sup>175–177</sup> Another challenge with collagen enthesis scaffold is the degradation rate. After being implanted, the structures and the biomechanical properties of collagen enthesis scaffolds inevitably deteriorate in a short time, which severely impacts its actual biofunctions.<sup>178–180</sup> Therefore, if the biocompatibility and the degradation rate of collagen enthesis scaffold could be improved, its applications for enthesis regeneration will become more widespread.

**Silk scaffolds.** Natural silk is a protein polymer produced by insects such as silkworms, scorpions, and spiders. Out of all the available silks, silkworm silk (Bombyx Mori silk), is the most widely used in the field of TE.<sup>181–183</sup> A key component of silk material is the silk fibroin (SF).

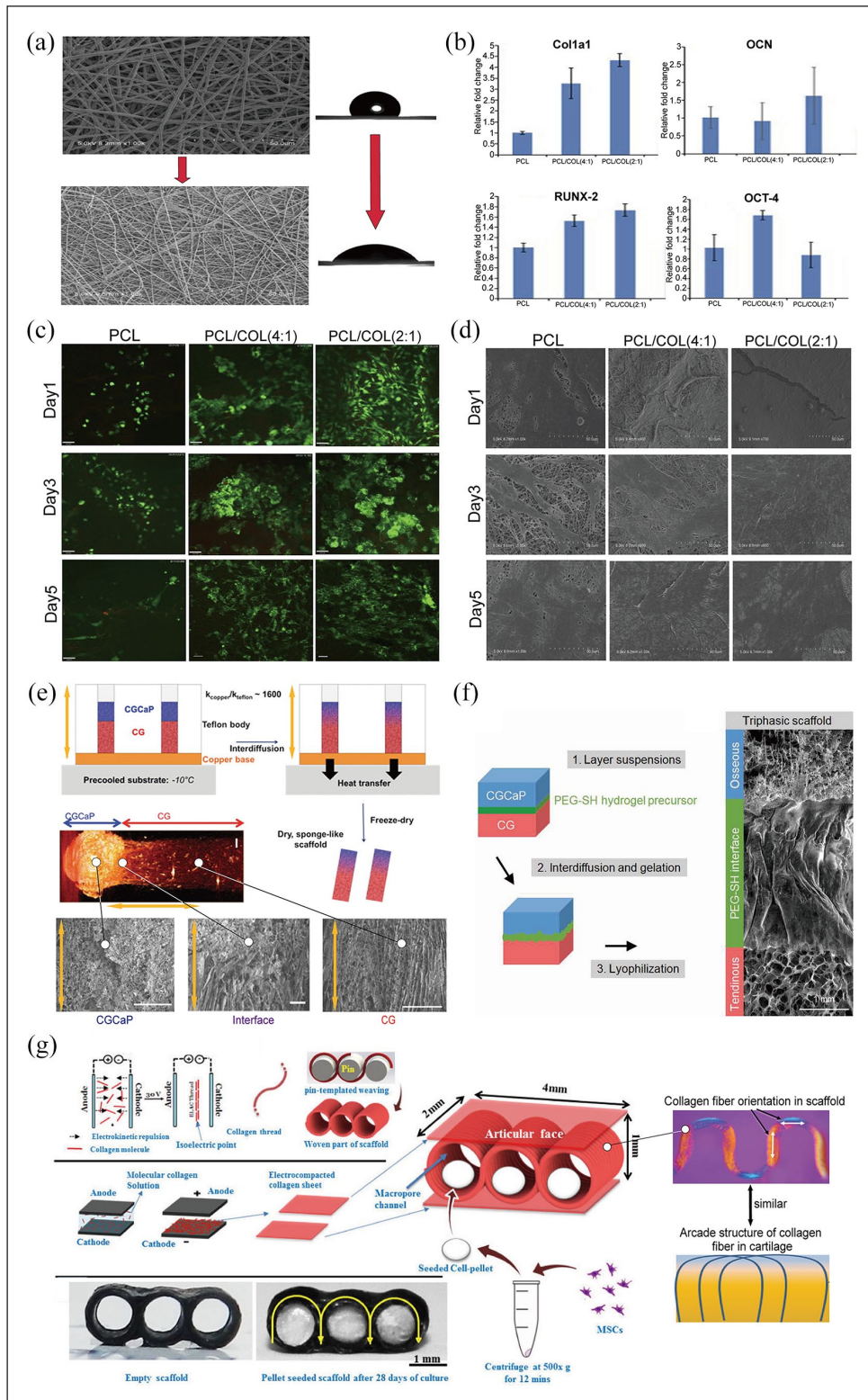


**Figure 4.** Addition of collagen material increased the porosity and hydrophilicity of the electrospun PCL scaffold (a), upregulated the osteogenic-related genes (Col1a1, OCN, RUNX-2, OCT-4) (b), enhanced the proliferation rate of TSPCs seeded in the scaffold (c) and conferred a widely-spread morphology (d).<sup>156</sup> (e–g) The different biomimetic collagen entheses scaffolds.<sup>160,161,165</sup>

PCL: poly ( $\epsilon$ -caprolactone); COL: collagen; CG: collagen and GAG; CGCaP: collagen, GAG and calcium phosphate; PEG: polyethylene glycol; MSCs: mesenchymal stem cells.

There are at least two major types of fibroins in the silk composition, which are referred to as the light chain (25 kDa) and the heavy chain (325 kDa). These two core biocompatible fibroin molecules constitute the composite silk fibers characterized by an anti-parallel  $\beta$ -sheet crystal conformation in space which confer the ideal mechanical properties to the silk material. Besides, a glue-like sericin protein coat binds the SF to reinforce the molecular structure of the silk fibers.<sup>184</sup> Before being utilized in the fabrication of the biological scaffold, the silk should be fully degummed, dissolved, dialyzed, and then centrifuged from the SF solution, which is the common source of material for silk scaffold fabrications.<sup>184–186</sup> Silk is a biocompatible material with ideal mechanical properties, and to uncover the possible applications of silk material in entheses TE, there have been many attempts on silk entheses scaffold to explore the influence on entheses regeneration.

For instance, in 2021, Chen et al. successfully manufactured a gradient-mineralized electrospun silk entheses scaffold. Briefly, a nanofibrous silk membrane was fabricated by an electrospinning device, and then the silk membrane was placed vertically in a  $10\times$  simulated body fluid (SBF) to produce a spatial decrease in mineralization degree from the bottom to the top of the silk membrane (Figure 5(a)). SEM images showed a regular topology from the bottom to the top of the scaffold, and the energy-dispersive X-ray spectroscopy (EDS) and Fourier transform infrared spectroscopy (FTIR) analyses further confirmed the existence of the gradient mineral deposition. These experiments demonstrated that the scaffold was highly like the native structure of the entheses tissue. Next, the osteochondral inductivity of this gradient-mineralized silk entheses scaffold was fully analyzed. Compared to the no-mineralized silk scaffold, the gradient-mineralized silk entheses scaffold could simultaneously promote both bone and cartilage tissue growth. Specifically, the area with higher degree of mineralization had larger osteogenic differentiation inductivity, while the area with lower degree of mineralization had more chondrogenic differentiation inductivity (Figure 5(b)). Due to these unique characteristics, the gradient-mineralized silk entheses scaffold can be applied to restore the natural composition of entheses tissue, which could fuel the regeneration of Zone II, Zone III and Zone IV.<sup>187</sup>

Besides trying electrospun silk entheses scaffold in entheses TE, there are attempts to explore salt-leached silk entheses scaffold for use in entheses regeneration. Although the manufacturing protocols are diverse, the overall fabricating processes of the salt-leached silk entheses scaffolds are nearly the same. Briefly, porogen particles (such as sodium chloride) are first added into the SF solution, soaked and dissolved in water, and then a porous silk scaffold is successfully leached out.<sup>188</sup>

Based on the fabrication process of salt-leaching, Yan et al. manufactured a Silk/Silk-nanoCaP bilayered salt-leached entheses scaffold. The whole scaffold had an

amorphous conformation, which presented a special macro/microporous interconnective topology that highly mimicked the entheses ECM. At the interface of the two layers, the transformation on the CaP content and scaffold porosity were gradient, and these two different layers proved to be perfectly integrated, which corresponded to the native region of Zone II and Zone III (Figure 5(c)). Both *in vitro* and *in vivo* experiments with this bilayered entheses scaffold showed that the Silk-nanoCaP layer had more osteogenesis and angiogenesis capacities, while the Silk layer had higher chondrogenesis capacity. In the Silk layer of the scaffold, there was more proliferation of chondrocytes in the normal round phenotype, more infiltration of cartilage tissue, and more generation of GAG and collagen type II. In the Silk-nanoCaP layer, newly-formed subchondral bones and vessels were fully observed, and the immunohistochemical staining showed presence of an angiogenic marker (SNA-lectin) (Figure 5(d)).<sup>189</sup> Therefore, this Silk/Silk-nanoCaP bilayered salt-leached entheses scaffold was demonstrated to be an efficient scaffold to be applied in entheses TE, which could enhance angiogenesis, osteogenesis and chondrogenesis in the entheses tissue. Besides the nanoCaP particles, glycerol can also be used in salt-leached silk scaffold to achieve higher entheses biomimetic degrees. In a study by Xiao et al. glycerol was added into the scaffold to manipulate the structural characteristics of the silk scaffold. SEM images revealed that the silk scaffold had a more amorphous structure in nano-scale that corresponded to the microstructure of native entheses after addition of the glycerol.<sup>190</sup> These findings showed that salt-leached silk scaffold could be another entheses scaffold used in entheses TE. Indeed, previous evidence showed that salt-leached silk scaffold might positively affect the process of neurogenesis.<sup>191</sup> Since the entheses and nerve injuries in the spine region often occur simultaneously, this scaffold could be more curative in the applications of spinal injuries.<sup>192,193</sup>

In addition to the electrospun and salt-leached silk entheses scaffolds, freeze-dried silk entheses scaffold is another potential silk scaffold in entheses TE. The overall fabricating process resembles that of the freeze-dried collagen scaffold, and a spongy-like porous silk scaffold can also be generated, which contains a splendid ECM-biomimetic inner architecture. The pore sizes of the freeze-dried silk scaffold usually vary from tens to hundreds of microns, and within reasonable range of modification, the higher freezing temperature can cause a larger pore size, demonstrating an ideal modulability.<sup>194,195</sup>

Based on the freeze-drying theories, Sang et al. designed a novel type of amorphous silk porous scaffold and fabricated it to explore its possible biofunction in angiogenesis of soft tissues. Through tuning of different freeze-drying temperatures from  $-20^{\circ}\text{C}$  to  $-5^{\circ}\text{C}$ , the researchers successfully produced a sequence of amorphous silk porous

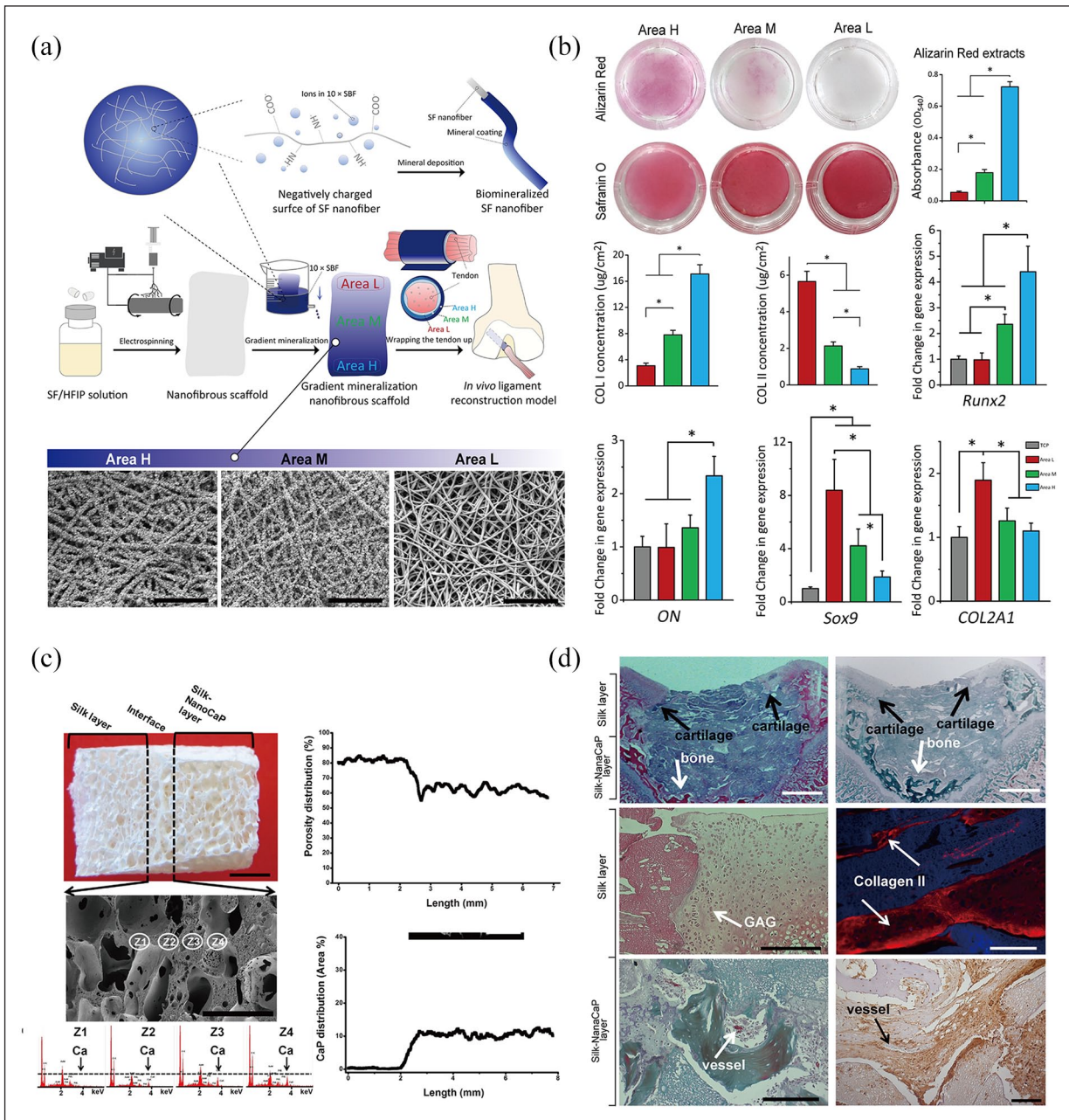


**Figure 5.** (a) The fabrication and structural layout of a gradient-mineralized electrospun silk enthesis scaffold.<sup>187</sup> (b) In the gradient-mineralized scaffold, areas with a higher degree of mineralization had more osteogenic differentiation inductivity (shown by Alizarin Red staining and the absorbance of staining extracts; collagen I concentration of cells seeded on the scaffold; gene expression levels of RUNX2 and ON) and lower chondrogenic differentiation inductivity (shown by Safranin O staining; collagen II concentration of cells seeded on the scaffold; gene expression levels of COL2A1 and Sox9).<sup>187</sup> (c) The structural characteristics of the Silk/Silk-nanoCaP bilayered salt-leached silk scaffold.<sup>189</sup> (d) Chondrogenesis capacity is higher in the Silk layer. Osteogenesis and angiogenesis capacities are higher in the Silk-nanoCaP layer.<sup>189</sup>

scaffolds. The amorphous silk porous scaffolds had similar ECM-mimicking inner microstructures, and analysis of scaffold characteristics revealed that the scaffold generated at the higher temperature had a slower degradation rate and a larger compressive modulus, which corresponded to better stability and better mechanical properties, respectively (Figure 6(a)). Furthermore, *in vitro* and

*in vivo* experiments showed that the scaffold produced at the higher temperature had great enhancements on the proliferation of MSCs, the growth of collagen content and the neovascularization capacity (Figure 6(b)–(d)).<sup>196</sup> Because the enthesis tissue is a collagen-rich composite tissue containing the soft tissue components in Zone I, Zone II and Zone III, this amorphous silk porous scaffold could also be

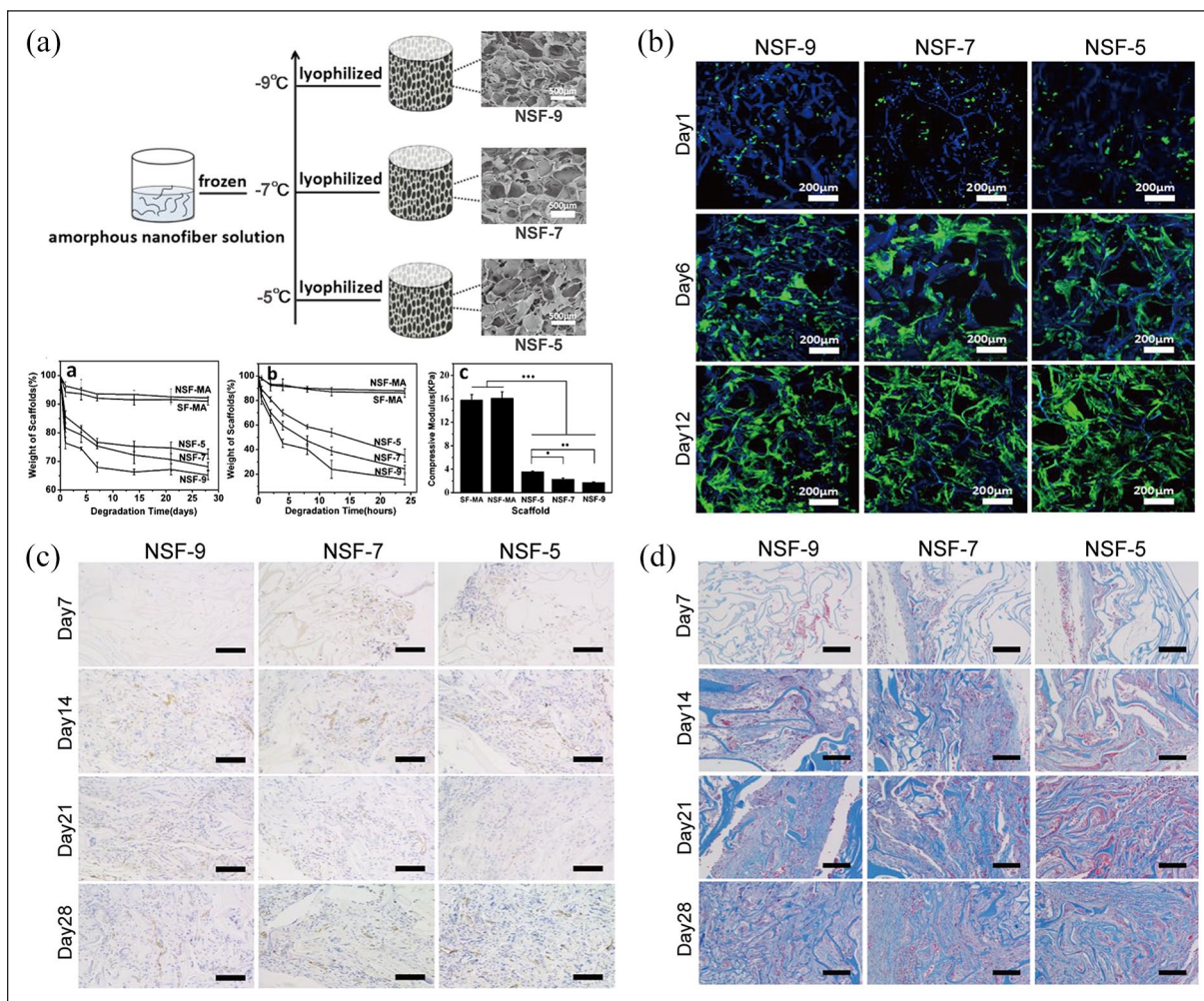


**Figure 6.** (a) A sequence of insoluble amorphous silk entheses scaffolds freeze-dried at different temperatures and their mechanical properties.<sup>196</sup> The scaffold produced at a higher temperature has faster cell proliferation rate (b), larger neovascularization capacity, (c), and more regeneration of collagen content (d).<sup>196</sup> NSF-9, insoluble scaffolds derived from amorphous silk nanofiber solution and frozen at  $-9^{\circ}\text{C}$ ; NSF-7, insoluble scaffolds derived from amorphous silk nanofiber solution and frozen at  $-7^{\circ}\text{C}$ ; NSF-5, insoluble scaffolds derived from amorphous silk nanofiber solution and frozen at  $-5^{\circ}\text{C}$ .

utilized for entheses regeneration. In addition, since the vascular network distribution is poorer in entheses tissue compared to other tissues, this silk scaffold is believed to effectively stimulate angiogenesis in the entheses regeneration process, which could tremendously enhance the regeneration of the injured entheses tissues. The inner architecture of this amorphous silk porous scaffold could be easily controlled by tuning the different fabricating temperatures, thus the scaffold might be feasibly used to produce a refined hierarchical entheses scaffold, which is stratified with multiple amorphous layers, which mimics the histological structures of the different regions of the entheses tissue. This amorphous silk porous scaffold has a big potential in entheses TE, and thus there is a need for more relevant research of this silk scaffold on entheses regeneration.

In summary, silk entheses scaffold is an ideal kind of a biological scaffold with great mechanical properties in

entheses TE. The properties include good strength, great toughness, and excellent elasticity, good biodegradability and bioresorbability. Besides, its main component, silk fibroin can be easily digested by proteases, yielding degradation products including amino acids or some small peptide molecules, which can directly be absorbed by body tissues. After being implanted, silk entheses scaffold is totally degraded and absorbed within a year with the participation of macrophages.<sup>197</sup> However, the silk entheses scaffold is still limited by few challenges which restrict its applications. Compared with the silk fibroin, the element of sericin is far less compatible with the human immune-system which could induce Type I allergic reaction in human bodies.<sup>198,199</sup> Although majority of the sericin component in silk material was removed in the preparation process of the SF solution, there could still be few sericin remnants which could act as an allergen in the entheses scaffold.<sup>198,199</sup> Moreover, in the silk scaffold fabrication

process, organic solvents or some harmful materials may inevitably be residual, which may increase the toxicity of the silk scaffold.<sup>200</sup> Therefore, there is a need to develop strategies to circumvent these problems associated with the application of silk entheses scaffold in entheses TE.

**HA hydrogel.** Apart from the above-described collagen and silk, the Hyaluronic acid (HA) biomaterial also draws a lot of attention in entheses TE. HA is a subunit of GAGs, which has a relatively looser molecular structure and a weaker mechanical property, thus it is mainly made into hydrogel and appended into other types of scaffolds. HA is a widespread molecule in various extracellular matrices of our human bodies, which is also an essential component of the entheses tissue. It can reinforce molecular connection of collagen fibers, increase histological viscoelasticity, and can function as a lubricant in collagen fibers to decrease friction and occurrence of fiber breakage.<sup>201</sup> Therefore, incorporation of entheses scaffold with HA could increase its mechanical properties and endurance. Frizziero et al. applied a repeated HA injection into the peri-Patellar tendon region of a detrained rat, and showed that HA could increase collagen I content, decrease collagen III content and could have a positive effect on maintenance of the entheses structure from detraining-associated damage.<sup>202</sup> Furthermore, HA is also an anti-inflammatory biomolecule. Addition of this element could lead to alleviation of the inflammatory response intrigued by the implanted scaffold, thus promoting the scaffold biocompatibility and exerting a positive effect in entheses regeneration.<sup>203–207</sup> Therefore, the HA hydrogel might be another promising natural biomaterial useful in entheses TE.

**Polyolefins and Poly (urethanes).** Conservative Polyolefins, such as poly tetrafluoroethylene and poly propylene were the initial synthetic polymeric biomaterials used in entheses TE. Initially, researchers focused on the restoration of the anatomy using the Polyolefin materials. They used these materials to reconnect the tear and gap or to refill the large void defect of the entheses and thus rebuild the histological completeness. There was no consideration of the cellular ingrowth or tissue regeneration, and the final outcomes did show many poor effects of these bio-inert materials: the maximum bearable tensile forces were weaker, external strengths could easily deform the implanted polymers, deterioration of injured entheses without any regeneration, and lack of any biodegradability for these biomaterials.<sup>208,209</sup> Because of these shortcomings, the Polyolefin materials were rendered obsolete.

Apart from the Polyolefins, researchers have also tried Poly (urethanes) in entheses TE due to their superior mechanical properties. Poly (urethanes) are polymers synthesized by condensation polymerization reactions between different isocyanates and polyols, which are usually accelerated by some catalysts or activated by UV radiation. Compared with Polyolefins, the tunability of the

Poly (urethanes) is slightly higher. By altering the different kinds or ratios of isocyanates and polyols, the molecular architectures and mechanical properties of these polymers become tunable.<sup>210–212</sup> The biggest advantage of the Poly (urethanes) is that the polymers have high tensile properties, which are capable of enduring large extensions without rupture. Besides, Poly (urethanes) have good elasticity and shape-memory properties, where they can recover to the primary shapes immediately following withdrawal of the tensile forces applied on the Poly (urethane) materials.<sup>213</sup> Due to these excellent mechanical merits, Poly (urethanes) are ideal synthetic polymeric biomaterials used to mimic the native tendon and ligament tissues. Furthermore, Poly (urethane) scaffolds have better bioactivities, with improved cellular adhesion and attachment on those materials.<sup>214,215</sup>

Although the overall properties of the Poly (urethane) scaffolds have tremendously increased compared to the conventional Polyolefin scaffolds, these scaffolds are still associated with some disadvantages. For instance, the cellular proliferating effects on their surface were not very satisfactory, and the cells seeded on Poly (urethane) scaffolds often have slow proliferation rates.<sup>216,217</sup> Moreover, the hydrophilicity of the Poly (urethane) scaffolds is not very well, and their biodegradability is still insufficient. Besides, the overall degradation rates of the Poly (urethane) scaffolds are quite slow: some *in vitro* analyses revealed that only around 12 wt % of the Poly (urethane) scaffolds was degraded at 37°C after 120 days, and around 21 wt % was degraded *in vivo* after 100 days.<sup>218</sup> Extension of time span of the *in vitro* experiment on Poly (urethane) degradation to 260 days did not significantly increase scaffold weight loss.<sup>219</sup> Furthermore, the degraded Poly (urethane) scaffolds could release some toxic organic products, which could potentially harm normal tissues and organs.<sup>220</sup> Therefore, the applications of Poly (urethanes) materials in entheses TE is partially limited.

**Poly (esters).** More investigations have unearthed more advantageous groups of synthetic polymeric biomaterials, and Poly (esters) are presently the most widely used biomaterials in entheses TE. Poly (esters) are synthetic polymers whose monomers are interconnected by ester groups produced from esterification reactions. In theory, Poly (esters) are hydrolysable due to existence of the ester groups. However, in practice, only a few kinds of Poly (esters) (e.g. the aliphatic Poly (esters)) possess better biodegradability and are capable of being used as biological scaffolds.<sup>221</sup> As of now, the Poly (esters) frequently-applied in TE are PLA (Polylactic acid), PGA (Polyglycolic acid), PCL (Poly( $\epsilon$ -caprolactone)), and PLGA (Polylactid-co-glycolid acid), and they are often fabricated into various scaffolds in form of Poly (esters) fibers.<sup>222–225</sup>

Among the Poly (esters), PLA draws our biggest attention because of its superior biocompatibility. PLA is a simple monomer synthesized organic polymeric biomaterial, which is only composed of lactic acid (LA) molecules.

Since LA is in the form of either L (levogyrate) or D (dextrorotatory) isomer, PLA can be further divided into PLLA (poly-L-lactic acid), PDLA (poly-D-lactic acid) or PDLLA (poly-D,L-lactic acid), whose molecular architectures and mechanical properties are slightly different.<sup>226–233</sup> As the main degradation products of PLA, LA is one of the most critical energy substrates besides glucose and aliphatic acids. These small molecules can be easily transported across the cytomembrane into the cellular plasm and participate in cellular anaerobic respiration.<sup>234–238</sup>

Based on its biosafety and biocompatibility characteristics, PLA is a superior biomaterial for enthesis TE applications. Indeed, Uehlin et al. found that aligned electro-spun PLLA nanofiber mats whose surfaces had been treated via controlled NaOH hydrolysis were a feasible scaffold for both cell adhesion and proliferation of hMSCs. This NaOH-treated PLLA scaffold had more enhanced osteogenic differentiation of hMSCs than untreated scaffolds. Furthermore, soaking this PLLA scaffold in bovine thrombin and fibrinogen not only added an extra layer of fibrin to its surface but also subsequently generated more connective topological structures within it resulting in decreased mobility of the PLLA fibers. This PLLA/fibrin hybrid scaffold had good mechanical properties, and due to the additional fibrin layer, it had an increased capacity for osteogenic differentiation (Figure 7(a)).<sup>239</sup> Thus, it is possibly applicable in enthesis TE as it can contribute to the mineralization process of enthesis regeneration. Relatedly, Li et al. fabricated a dual-layer organic/inorganic bipolar PLLA enthesis scaffold with an electro-spinning device. The layers were from pure PLLA and nano-hydroxyapatite-PLLA fibers to simulate the non-mineralized and mineralized enthesis regions respectively (Figure 7(b)). Their simulated body fluid (SBF) mineralization-inducing *in vitro* experiment showed the good mineralization capacity of the nHA-PLLA layer (Figure 7(c)). This bipolar enthesis scaffold significantly increased, *in vivo*, GAG formation and collagen generation in regenerated enthesis tissues (Figure 7(d)–(f)).<sup>240</sup> Based on its favorable fibrogenesis, chondrogenesis, osteogenesis, and inductive capacities, it is most applicable in enthesis TE.

Apart from PLA, other biodegradable materials used in enthesis regeneration are PGA, PLGA, and PCL. Low molecular weight PCL debris are safe, and permeate blood microvessels for transportation to the kidney and liver, from where they are excreted via urine and bile respectively.<sup>241,242</sup> For both PGA and PLGA, glycolic acid is the main degradation product, which is then oxidized to glyoxylic acid that enters the human tricarboxylic acid cycle. Therefore, these biodegradable biomaterials are applicable in enthesis TE. Cao et al. manufactured a PCL/PCL-tricalcium phosphate (TCP) /PCL-TCP multi-layered porous scaffold via a three-dimensional (3D) printing device, which mimicked the natural tendon-fibrocilage-bone histological multilayers of the enthesis tissue

(Figure 8(a)). This scaffold was designed with three different layers that corresponded to the composition and thicknesses of Zone I, Zone II-Zone III, and Zone IV of native enthesis tissue and thus primarily giving it biomimetic characteristics. Indeed, it promoted fibrogenesis and chondrogenesis, cell proliferation, and ECM deposition that was spatially distinct among the three layers (Figure 8(b)).<sup>243</sup> Romeo et al. implanted a PGA/poly-L-lactide-co- $\epsilon$ -caprolactone (PLCL) nanofiber scaffold at the rotator cuff tendon enthesis site of a sheep, and after a period of 12 weeks, the native enthesis tissue structures successfully recurred in the scaffold-treated group.<sup>42</sup> Relatedly, Smith et al. fabricated a porous PLGA scaffold via salt-leaching and etched it with NaOH to modify its surface topography. The resultant scaffold had higher porosity and rougher nano-surface topography than unetched PLGA scaffolds, and this corresponded to the typical tissue structure of Zone IV (Figure 8(d)).<sup>244</sup> The adhesion of osteoblasts on it significantly increased, whereas that of fibroblasts decreased (Figure 8(e)). Thus, this special NaOH-etched PLGA scaffold is likely to improve Zone IV regeneration whereas the unetched PLGA scaffold would be beneficial for regeneration of Zone I in enthesis TE applications — fabricating a curative multi-layered PLGA scaffold for enthesis regeneration is a worthwhile venture.<sup>244</sup> Furthermore, Eriskin et al used a new processing method of twin-screw extrusion/electrospinning (TSEE) to fabricate a special PCL scaffold with a continuously-increasing amount of  $\beta$ -tricalcium phosphate in its inner structure that was similar to the native structures of Zones II and III of enthesis tissues.<sup>245</sup> Using the same method, they fabricated a similar insulin/PCL/ $\beta$ -glycerophosphate scaffold, which contained simultaneous gradients of increasing and decreasing insulin and  $\beta$ -glycerophosphate respectively. Its insulin- and  $\beta$ -glycerophosphate-rich regions had high capacities for chondrogenesis and osteogenesis respectively.<sup>246</sup> Thus, this scaffold is also applicable in enthesis TE—it would predominantly effectively enhance regeneration in Zones II and III.

Taken together, synthetic polymeric scaffolds can be effectively applied in enthesis TE as they have higher degrees of tunability and reproductivity, and better biosafety profiles—since they lack potential inherent antigens/pathogens—than naturally-sourced enthesis ones.<sup>108,247,248</sup>

Biological strategies are considered a most critical aspect of enthesis TE. For example, the use of biological scaffolds provides a biomimetic platform that gives a bio-active environment for the regeneration and infiltration of the injured enthesis tissue. Thus, enthesis scaffolds should be designed and fabricated with either three layers that correspond to the tendon, fibrocilage, and bone or four layers that correspond to the tendon, unmineralized fibrocilage, mineralized fibrocilage, and bone. Moreover, to better emulate the native structures of Zones II and III,

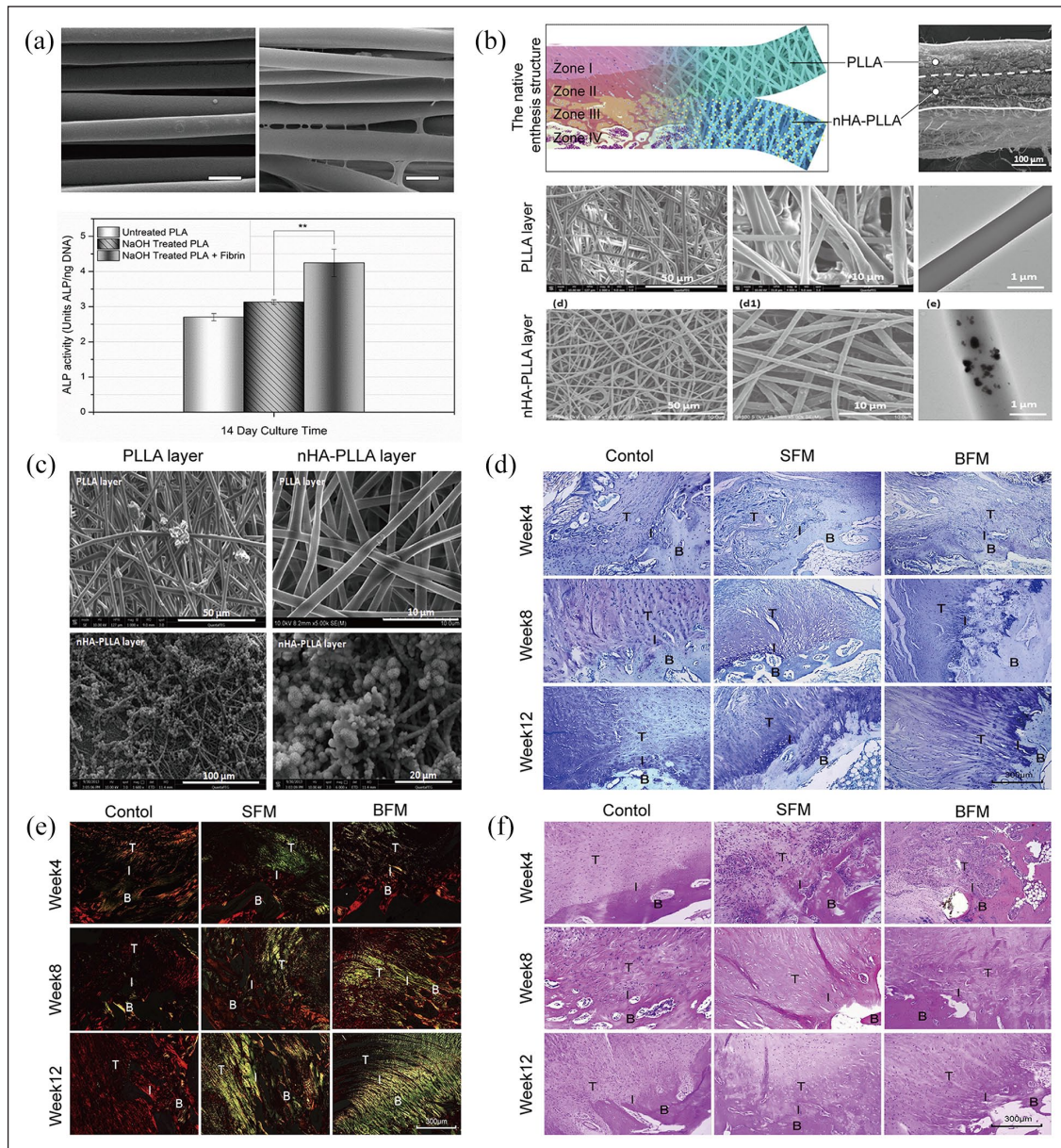


**Figure 7.** (a) With an extra layer of fibrin coated, more connective topological structures were generated, and the osteogenic differentiation capacity was elevated compared to the non-coated PLLA scaffold.<sup>239</sup> (b) The structure of bipolar PLLA/nHA-PLLA enthesis scaffold,<sup>240</sup> (c) The nHA-PLLA layer had the larger mineralization capacity compared with the PLLA layer.<sup>240</sup> The elevated GAG formation (d), collagen formation (e), and enthesis tissue regeneration (f) in the dual-layer enthesis scaffold were proved via the histological stainings.<sup>240</sup>

PLLA: poly-L-lactic acid; nHA: nano hydroxyapatite; T: tendon; I: interface; B: bone; SFM: simplex fibrous membrane of PLLA; BFM: bipolar fibrous membrane of PLLA/nHA-PLLA.

enthesis scaffolds with inner structures and topologies that have gradients are indispensable.

### Cell strategy

Enthesis-related cells are applicable in promoting enthesis regeneration and this is the basis of cell strategies in enthesis TE. Such cells include osteoblasts, fibroblasts, costal-cartilage-derived stem cells (CDSCs), tendon stem/

progenitor cells (TSPCs), adipose-derived stem cells (ADSCs), and mesenchymal stem cells (MSCs). The specific effects of these cells in enthesis TE have been previously investigated.

Cooper et al. seeded opposite ends of a commercially purchased PLA scaffold with both osteoblasts and fibroblasts which were then co-cultured. The GAG and collagen contents of the ECM in the fibroblasts, osteoblasts, and transition regions were then assessed,



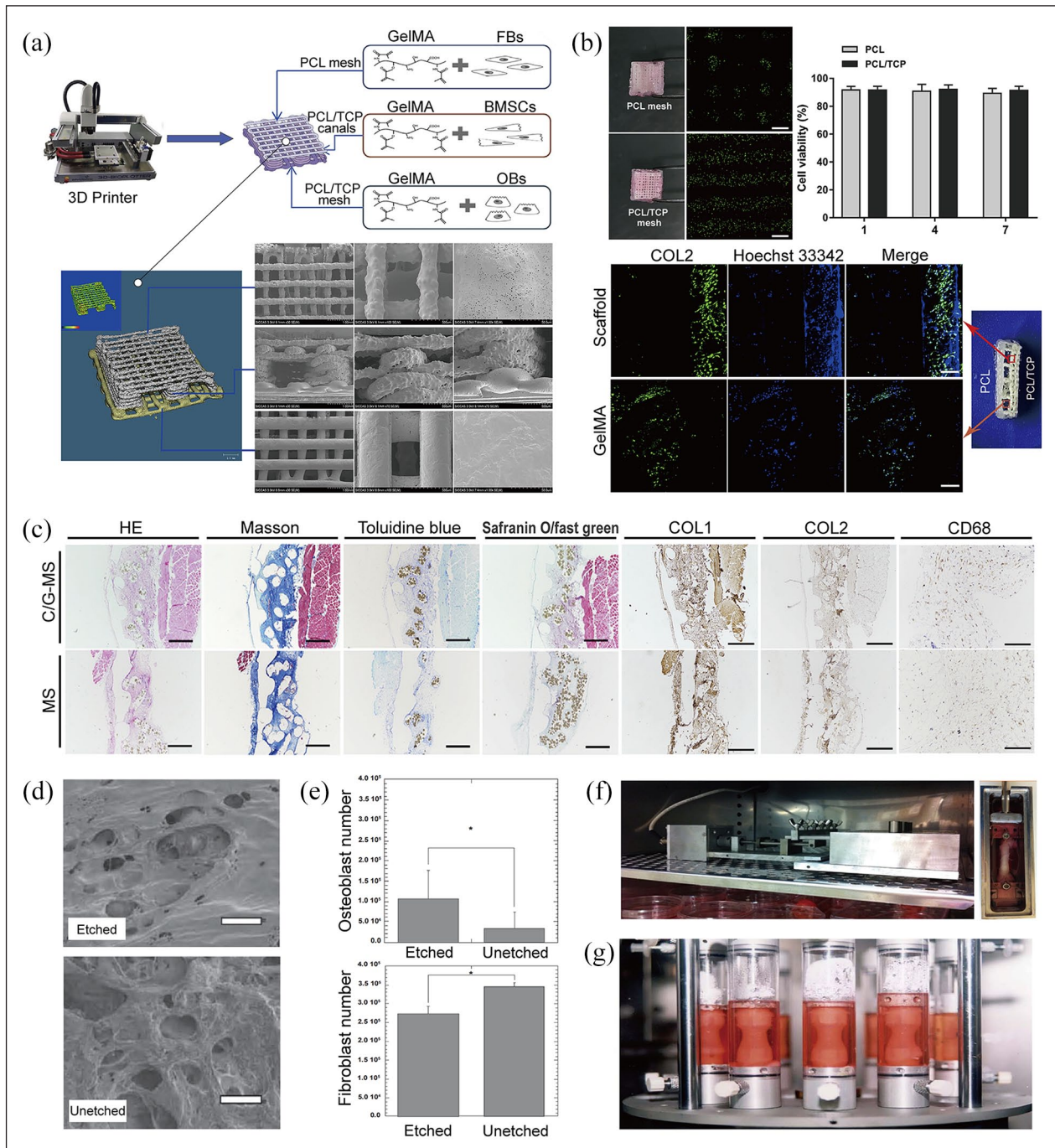


**Figure 8.** (a) A triphasic 3D-printed enthesis scaffold mimicking the natural tendon-fibrocartilage-bone structure of enthesis tissues.<sup>243</sup> (b) The cell proliferation and ECM deposition were high in the PCL/TCP layer.<sup>243</sup> (c) Histological stains showing improved regeneration of enthesis tissues due to the 3D-printed enthesis scaffold, and elevation of positive effects due to loading with GelMAs (containing either fibroblasts, BMSCs, or osteoblasts).<sup>243</sup> (d) After NaOH etching, the PLGA scaffold had high porosity and rough nano-surface topography that both corresponded to the tissue structure of Zone IV (Bone).<sup>244</sup> (e) The adhesion of osteoblasts increased, whereas that of fibroblasts simultaneously decreased in the NaOH-etched PLGA scaffold.<sup>244</sup> (f and g) The two different kinds of bioreactors that were used to apply cyclical stress stimulations on tendons.<sup>274,275</sup> PCL: poly( $\epsilon$ -caprolactone); TCP: tri-calcium phosphate; GelMA: gelatin methacrylate; PLGA: polyglactin.

and they were generally higher in the fibroblast region—the transition region between the two cellular regions mostly had intermediate values of the GAG and

collagen contents at different time points. Thus, fibroblasts promoted effective ECM deposition on the enthesis scaffold and co-culturing fibroblasts with

osteoblasts contributed to the formation of the natural gradient of the enthesis ECM.<sup>249</sup>

Zuo et al. successfully harvested CDSCs from the costal cartilage tissue of newborn Sprague-Dawley rats and showed that these cells had ideal proliferation abilities and cell viability under low oxygen and nutrient *in vitro* conditions. This corresponds to the environment of injured enthesis tissues. The CDSCs-hydrogel was then wrapped with a decellularized tendon scaffold, and this was transplanted into a defective rat patellar tendon enthesis, wherein the CDSCs survived, proliferated, and differentiated into osteocytes, chondrocytes, and tenocytes. Typical tendon-fibrocartilage-bone histological structures recurred in the regenerated enthesis tissues, and the biomechanical properties (failure load and tissue stiffness) of the repaired tissue were significantly higher than that of the control.<sup>131</sup> This supports the hypothesis that CDSCs are highly applicable in enthesis TE.

To elucidate possible functions of TSPCs in the regeneration of enthesis, Shen et al. produced a knitted silk/collagen sponge scaffold seeded with additional TSPCs and then transplanted it into a defective rabbit rotator cuff tendon enthesis. More fibroblast growth, less lymphocytes infiltration into the regenerated enthesis tissue and scaffold, and denser deposition of ECM and collagen were observed in the TSPCs-seeded scaffold than in the control. Moreover, nascent collagen fibers were more continuous and homogeneous, the interfaces between scaffold and enthesis tissues were more aligned, and higher overall mechanical properties in regenerated enthesis tissues were observed in the TSPCs-treated group than in the control. Relatedly, the expression level of fibrogenic genes (collagen I, collagen III, DCN) in TSPCs-treated scaffold was significantly upregulated, corroborating the positive effect of TSPCs on the fibrogenesis in enthesis tissue regeneration. As lymphocyte infiltration was inhibited in this scaffold, TSPCs possibly have an anti-inflammatory effect during regeneration of enthesis.<sup>250</sup>

For ADSCs, McGoldrick et al. seeded a decellularized-enthesis scaffold with ADSCs and then used it—or a blank enthesis scaffold without ADSCs seeded—to reconstruct rat Achilles tendon enthesis tissues. The regenerated Achilles tendon enthesis in the cell-seeded group had superior biomechanical properties—ultimate failure load, ultimate tensile stress, stiffness—more tendon and fibrocartilage tissues within the scaffold, and more collagen type III in the extracellular matrices than the unseeded group. Thus, ADSCs possibly promoted enthesis regeneration in injured enthesis tissues via fibrogenesis and chondrogenesis processes.<sup>251</sup> In a related study, Zhao et al. co-cultured ADSCs with injured tenocytes for 48 h, ADSCs clearly promoted proliferation rates and largely reduced levels of oxidative stress in the injured tenocytes via inhibition of methylation LncRNA Morf411.<sup>252</sup> Therefore, it is hypothesized that ADSCs mainly target the regeneration

of Zone I in the injured enthesis tissue, and exert their positive effect through LncRNA Morf411 demethylation.

Due to their totipotency, MSCs are not only widely medically utilized but are also specifically applied in repairing injured enthesis tissues, where a complex and simultaneous regeneration of multiple tissues is required. Nourissat et al. cut off a rat Achilles tendon and destroyed its enthesis. The free end of the tendon was then attached to the left bony tunnel with the fixation of sutures. They then either injected chondrocytes or MSCs into the repair site and evaluated their effects separately. These cell therapies were indeed efficient in reconstructing the injured enthesis—MSCs were even better than chondrocytes in improving high-level enthesis regeneration.<sup>253</sup> This was corroborated by Lim et al. who transplanted tendon autografts in rabbit ACL enthesis, and the reconstructed ACL was artificially coated with MSCs in a fibrin glue carrier. MSCs treatment group had larger areas of chondral regenerated in enthesis tissues than the control group, and a gradient transition from the cartilage to bone region was also observed. Thus, MSCs could intervene in the cartilage regenerating process of the injured enthesis tissue, which could greatly promote the maturation of enthesis tissues.<sup>254</sup> Using a 3D-printed triphasic enthesis scaffold, Cao et al. loaded three different gelatin methacrylates (GelMAs) encapsulating fibroblasts/BMSCs/osteoblasts onto the tendon, fibrocartilage, and bone mimicking layers. These applications of additional enthesis cells promoted fibrogenesis, chondrogenesis, and osteogenesis in the different layers of the complex enthesis scaffold (Figure 8(c)).<sup>243</sup> Therefore, MSCs possibly played an important role in the regeneration of enthesis tissues, which mainly acted in the cartilage regions of Zone II and III.

As another key strategy in enthesis TE, cell strategy mainly focuses on the additional applications of enthesis-related cells in enthesis tissues or scaffolds to further improve the regeneration of injured enthesis. Traditionally, enthesis-related cells were directly applied to the injured site of the enthesis tissue. However, the number of these cells, and their concomitant healing effects at the site, decreases with time. Thus, fixing enthesis-related cells on the enthesis scaffold to specifically act on the injured region may ensure longer-lasting effects. Hence, a current challenge in the successful application of cell strategy in enthesis TE is combining enthesis-related cells with the scaffold without diminishing their bioeffects.

### Growth factor strategy

Biological factors accelerate enthesis regeneration; more specifically growth factors have been applied in enthesis TE.<sup>34</sup> Currently, commonly-used growth factors include BMPs (bone morphogenetic proteins), FGFs (fibroblast growth factors), TGFs (transforming growth factors), GDFs (growth and differentiation factors), PDGFs

(platelet-derived growth factors), and VEGF (vascular endothelial growth factor). The possible functions of these factors in accelerating enthesis regeneration have been investigated.

Hashimoto et al. induced a tendon/ossicle complex by injecting BMP-2 into the rabbit flexor digitorum communis tendon enthesis and subsequently transplanted it onto the rabbit tibia surface. A month later, it had merged completely with the tibia and a direct insertion of a tendon-bone structure was histologically observed, corroborating the positive effect of BMP-2 in enthesis repairing.<sup>255</sup> For FGF-2, Yonemitsu et al. clearly demonstrated that FGF-2 elevated the degree of tenogenic regeneration for chronic rotator cuff enthesis tears in rats.<sup>256</sup> In order to explore the specific function of TGF- $\beta$ 3, Kovacevic et al. applied a calcium-Phosphate matrix—supplemented with TGF- $\beta$ 3—at the surgically-reconnected tendon-bone interface of a rat supraspinatus tendon enthesis. TGF- $\beta$ 3 tremendously enhanced the mechanical endurance as well as the generation of collagen in the repaired enthesis tissue.<sup>257</sup> Relatedly, Holladay et al. showed that the expression of tenogenic-related genes (DCN, SCX, collagen I) in TSPCs was largely upregulated by GDF-5 treatment—this indicated a potential fibrogenic effect of GDF-5 molecules in enthesis TE.<sup>258</sup> To elucidate the role of PDGFs in enthesis TE, Cheng et al. added PDGFs nanoparticles into a biomimetic collagen scaffold and showed that the ADSCs seeded onto this hybrid scaffold had a higher proliferation rate and a higher degree of tenogenic differentiation degree than the control. Thus, PDGFs had a stimulating effect on the regeneration of Zone I in enthesis tissue.<sup>259</sup> Furthermore, Cheng et al. showed that the Mg interference screw promoted enthesis fibrocartilaginous regeneration via VEGF endocellular accumulation, which corroborated the positive effect of VEGF in enthesis TE.<sup>260</sup>

The aforementioned factors all promoted enthesis regeneration, albeit via different mechanisms. For example, FGFs mainly target the fibrous region to promote the degree of fibrogenesis in enthesis tissues, whereas BMPs target both the chondral and bony regions to promote chondrogenesis and osteogenesis respectively.<sup>255,256</sup> TGF- $\beta$ 1 primarily promoted chondrogenesis in enthesis, whereas TGF- $\beta$ 3 simultaneously promoted fibrogenesis and chondrogenesis.<sup>261–263</sup> Therefore, for optimum enhancement of enthesis regeneration, two or more kinds of growth factors should be applied simultaneously, successively, or even iteratively in accordance with the different phases of enthesis healing.<sup>130,264,265</sup> Notably, heparin effectively reduced the release rate of TGF- $\beta$ 2 and GDF-5 from the enthesis scaffold and significantly increased their validity, which reinforced their fibrogenesis and chondrogenesis activities during enthesis regeneration.<sup>266</sup> Thus, heparin is a possible general potentiator of the beneficial effects of these growth factors in enthesis TE.

Taken together, the growth factor strategy is key for enthesis TE. Growth factor supplementation promotes the process of enthesis regeneration in injured enthesis tissues. Similar to the cell strategy, the growth factors are applied directly at the injured site of the enthesis tissue, which also reduces the prospects of long-lasting effects. Relatedly, the local injection of growth factors could not only cause an acute blood surge but also have unpredictable effects on normal tissues due to increased blood circulation of growth factor molecules. Therefore, growth factors should also be used in combination with enthesis scaffolds, not only to improve their targeting abilities but also to modulate their release.

### Biophysical modulation strategy

Both eccentric and concentric overload training promote enthesis healing in clinical practice.<sup>267</sup> Therefore, biophysical modulation might be a key intervention in the whole healing process of enthesis tissues.<sup>268–272</sup> Wang et al. invented a mechanical bioreactor to test the influence of stress stimulation on enthesis tissues *in vitro*. A full-length rabbit Achilles tendon was dissected and attached to the bioreactor. Then, the bioreactor was filled with culture medium maintained at the specific amplitude and frequencies so as to apply a tunable cyclical stress stimulation on this dissected tendon. Their stimulations showed that a 6% cyclic tensile strain was appropriate to maintain histological homeostasis in the Achilles tendon.<sup>273</sup> Additionally, they stimulated Achilles tendons with 6% strain, 0.25 Hz, 8 h/day for ca. 6 days (Figure 8(f)). This dynamically stimulated tendon had stronger mechanical properties and lower degradation rates than the static group. It also had decreased apoptotic cell ratios, more abundant and better-orientated collagen fibers, upregulated collagen generation-related genes (COL1A1, COL3A1, TGF- $\beta$ ), and significantly downregulated ECM degeneration-related genes (MMP-1, MMP-3).<sup>274</sup> These corroborated extra-applied dynamic stress stimulations as beneficial to the healing of enthesis tissues. In a correlative study, Altman et al., created a similar dynamic bioreactor and inoculated it with a collagen scaffold seeded with BMSCs (Figure 8(g)) and then maintained it at composite mechanical cyclic motion (10% translational strain, 25% rotational strain, 0.0167 Hz) for about 21 days. The scaffold had more nascent collagen fibers aligned along the axis of motion than the static-cultured scaffold—collagen fibers here were scarce and randomly oriented. Moreover, there was more cell division under this mechanical stimulation, and the ratio of the cells with either elongated or ligament-like morphology—which were also along the direction of mechanical loading—increased. Lastly, the expression of typical enthesis genes (Collagen Type I, Collagen Type III, tenascin-C) was tremendously upregulated under this stress stimulation.<sup>275</sup>

Simple static tensile forces have also been applied on enthesis scaffolds to promote enthesis regeneration. Rinoldi et al. fabricated a loop-like wet-spun gelatin methacryloyl (GelMA)-alginate scaffold encapsulated with BMSCs and then stretched it in the opposite direction with a bespoke stretching device so that the scaffold was subjected to 15% static strain. This static stress stimulation promoted cell proliferation, alignment, and the expression levels of some enthesis-related genes (Collagen Type I, Collagen Type III, SCX, TNMD).<sup>276</sup> Thus, both dynamic and static stress stimulations improved enthesis regeneration, and stress stimulation is key for the biophysical modulation strategy.

The use of electromagnetic fields is another key aspect of the biophysical modulation strategy. Pulsed electromagnetic fields (PEMF) not only improved the early healing of rat rotator cuff enthesis after reconstruction<sup>277</sup> but also promoted osteogenesis at the enthesis site to create a tight tissue connection at the tendon-bone interface.<sup>278</sup> However, there exists a paucity of studies on electromagnetic fields for enthesis TE and its mechanism of action remains to be clarified. That said, the biophysical modulation strategy is most advantageous since biophysical stimulations of the injured enthesis are usually uncomplicated and easily controllable, non-invasive, and repeatable, making it the most economic strategy for prospective clinical applications.

## Conclusions and future perspectives

In summary, the enthesis is a special complex tissue that is hard to regenerate. To achieve the successful regeneration of enthesis, the issues of tendon/ligament, cartilage and bone regenerations should all be considered at the same time, and these three kinds of tissues should be regenerated orderly in space corresponding to the composition of enthesis tissue. Due to developments in enthesis TE, four effective strategies (biological scaffold strategy, cell strategy, growth factor strategy, biophysical modulation strategy) have been unveiled so far to promote the regeneration of injured enthesis tissue significantly. And for achieving the best result of enthesis regeneration as we could, these strategies should be applied comprehensively.

Primarily, a special enthesis scaffold with the multifunction of fibrogenesis-chondrogenesis-osteogenesis is needed to be implanted *in situ* (fixed with sutures or screws). This scaffold should be designed and fabricated into multilayers. Different layers have the different biomimetic structures, which take the different duties on the regenerations of tendon/ligament, cartilage and bone. With this enthesis scaffold applied, an initial reconnection of the broken enthesis tissue could be established, and a biocompatible platform for the orderly ingrowths of the different types of tissues (tendon/ligament, cartilage and bone) could be provided, which would induce the recurrence of native enthesis tissue at last. In order to further elevate the

biofunction of enthesis scaffold, the enthesis-related cells and growth factors could both be applied additionally. Based on their specific characteristics, the different cells and growth factors should be laden into the different layers of enthesis scaffold. For example, ADSCs mainly act on the fibrogenesis and chondrogenesis processes of enthesis regeneration, and they should better be added into the fibrogenic and chondrogenic layers of enthesis scaffold. And for another example, BMPs mainly target at the chondral and bony regions of enthesis to promote chondrogenesis and osteogenesis, and they should better be added into the chondrogenic and osteogenic layers of enthesis scaffold (Figure 9). Furthermore, after the injured enthesis is repaired by the enthesis scaffold with cells and growth factors added, the static/dynamic forces and magnetic field could also be applied on the reconstructed enthesis tissue, which could promote the maturation process of the newly regenerated enthesis tissue effectively (Figure 9).

With all the strategies synthetically applied, the problem of enthesis regeneration has been improved tremendously in comparison with the traditional surgical treatments. However, there is still no method that results in the complete reemergence of intact and native enthesis tissues, necessitating the more improvements in enthesis TE in the future. As the most important component of enthesis tissue engineering, the biological scaffold strategy mainly focuses on designing, fabricating, and verifying the enthesis scaffold in the different biomaterials. Besides the general criteria of biodegradability, biocompatibility, biosafety and reproducibility for the production of biological scaffold applied in TE, an enthesis scaffold should meet the following criteria additionally:

(a) Enthesis scaffold should be designed with a tendon/ligament-cartilage-bone multiphasic biomimetic structure, and the interfaces between the different layers should preferably correspond to the specific interfaces between the native Zones of enthesis tissue so that the scaffold biomimetic degree can get established. The structural transition in the enthesis scaffold should be distinct and graded in the interfaces between fibrogenic and chondrogenic layers as well as chondrogenic and osteogenic layers, while at the same time, there should also exist a continuous structural gradient in the chondrogenic layer to emulate the natural structure from Zone II to Zone III.

(b) As a special biological scaffold applied at the complex tissue of enthesis, the overall mechanical properties of enthesis scaffold should be optimized to endure the external tensile forces and compressive forces without deformation. The specific mechanical properties of the different layers should also strictly correspond to the native Zones of enthesis tissue, which means that enthesis scaffold should be designed into a soft-hard transitioned scaffold. The soft terminal corresponds to Zone I, it should have the mechanical properties similar to the tendon/ligament tissue to endure the external tensile forces. The hard terminal

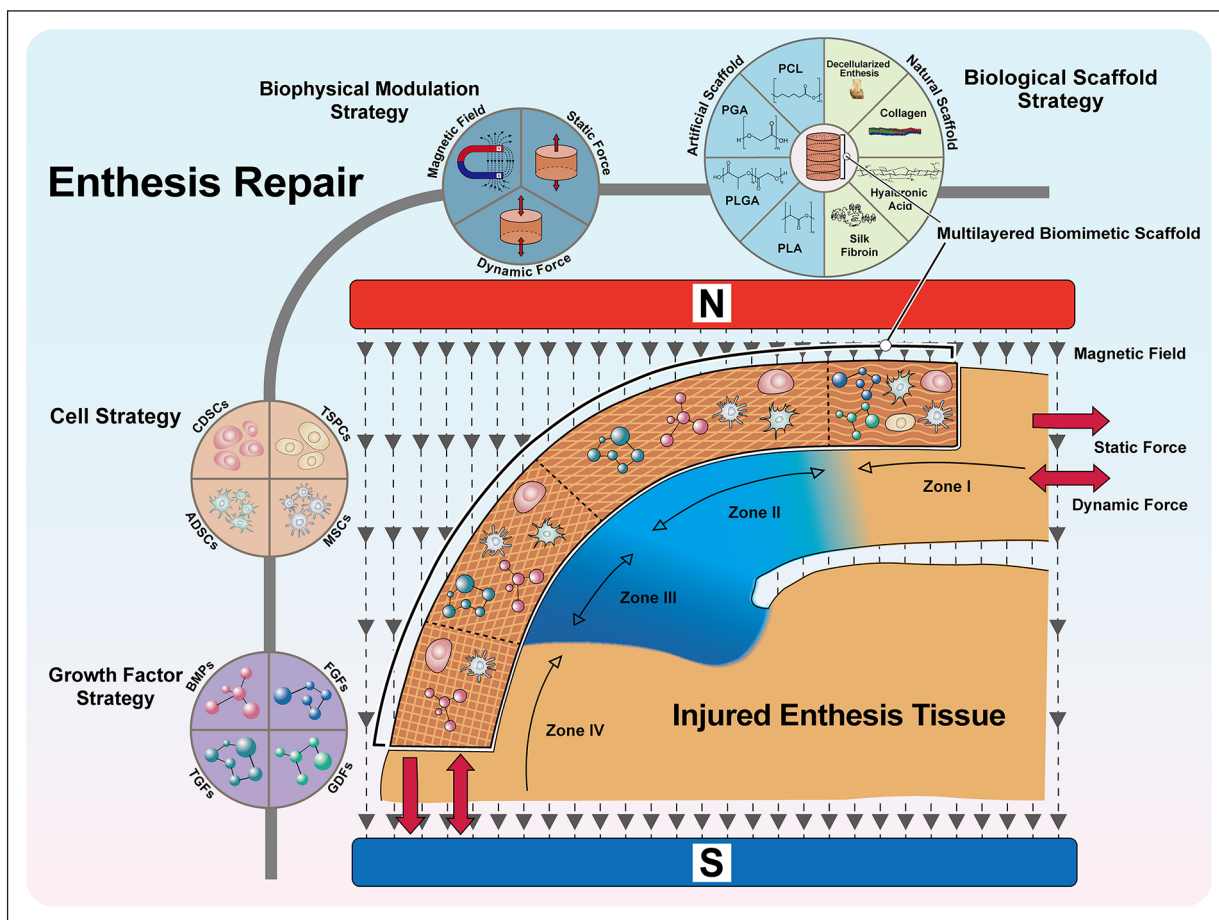


**Figure 9.** The schematic figure of different strategies' applications in entheses TE. To better regenerate the injured enthesis tissue, a multilayered biomimetic scaffold with the biofunction of fibrogenesis-chondrogenesis-osteogenesis should be implanted *in situ*. Each layer of the scaffold has the similar structure to the specific Zone contacted, which contains the fibrogenic, chondrogenic or osteogenic capacity to induce the regeneration of tendon/ligament tissue, cartilage tissue or bone tissue, respectively. Based on the spatial order of the specific biofunctions of the different layers in enthesis scaffold, different cells and growth factors could be laden into the targeting layers to further elevate the fibrogenic, chondrogenic and osteogenic capacities before the scaffold being implanted. After the reconstruction of the injure enthesis tissue with the enthesis scaffold, static/dynamic forces and magnetic field could be applied additionally, which could provide the extra mechanical stimulations to promote the maturation process of the newly-regenerated enthesis tissue effectively. With all these strategies being applied, a primitive enthesis tissue composed of tendon/ligament-cartilage-bone tissues could possibly reappear, which would turn into the native enthesis tissue after the long period of remodeling in the future.

CDSCs: costal-cartilage-derived stem cells; TSPCs: tendon stem/progenitor cells; ADSCs: adipose-derived stem cells; MSCs: mesenchymal stem cells; BMPs: bone morphogenetic proteins; FGFs: fibroblast growth factors; TGFs: transforming growth factors; GDFs: growth and differentiation factors.

corresponds to Zone IV, it should have the mechanical properties similar to the bone tissue to endure both tensile and compressive forces. The immediate part corresponds to Zone II and Zone III, it should have the mechanical properties similar to the cartilage tissue to endure both tensile and compressive forces as well.

(c) Apart from the structural and biomechanical requirements listed above, there is also another requirement about the biofunction of enthesis scaffold. The spatial order of biofunctions in enthesis scaffold should be followed as fibrogenesis-chondrogenesis-osteogenesis strictly. All the choices of biomaterials, cells and growth factors for the synthesis of enthesis scaffold should be based on this

requirement so that the primitive enthesis tissue could be regenerated under the induction of enthesis scaffold.

As we know, the proliferation and differentiation of cells can be influenced by the biomaterials on which they are attaching. Therefore, biomaterials that promote fibrocytes/chondrocytes/osteocytes should be used orderly to synthesize a multi-composed enthesis scaffold so that it could promote enthesis regeneration more effectively. In addition, some spatial properties in biological scaffolds (such as the porosity, pore size and the micro-topology) can also influence the cellular behaviors of the different cells and affect fibrogenesis/chondrogenesis/osteogenesis process. If these influencing factors are unveiled and

applied in the design&fabrication of enthesis scaffold, the utility of enthesis scaffold in enthesis TE will come to a much higher level in the future.

For the cell strategy in enthesis TE, the MSCs are the most common cells seeded on enthesis scaffold. Due to their multiple differentiation directions, MSCs in different layers of enthesis scaffold may be transformed into corresponding differentiated cell types in an ideal case. However, in actual practice, this regular fibrogenic/chondrogenic/osteogenic differentiation in the intended layer of scaffold is difficult to achieve. In our view, orderly seeding of fibroblasts, chondroblasts, and osteoblasts on different scaffold layers might be a better strategy for promoting enthesis regeneration. What's more, a combination of stratified enthesis scaffold and stratified cell seeding can enhance the regeneration of enthesis to a large degree.

To date, several biological molecules that promote the regeneration of enthesis have been investigated, especially focusing on growth factors. However, other molecules (e.g. some hormones and gene molecules) have not been researched. Therefore, further studies are needed to test the performance of hormone therapy and gene therapy in enthesis TE. Among the growth factors studied so far, most are used singly in enthesis TE and mostly target a single region of enthesis tissue, although enthesis regeneration involves at least three kinds of tissues (tendon/ligament, fibrocartilage and bone) at the same time. Therefore, we believe that two or more growth factors should be simultaneously laden onto the different layers of the enthesis scaffold to promote the regeneration of the intended tissues at the corresponding layers, hence improve the overall regeneration of the injured enthesis tissue.

Both the dynamic/static stress stimulation and electromagnetic field have been demonstrated as two types of valid biophysical modulation strategies for enthesis regeneration. However, they have not been sufficiently explored, and the methods utilized in the past experiments are have some practical limitations. Similarly, the role of stress stimulation in enthesis TE need to be further refined. The bioreactors used to apply mechanical forces are mostly custom-made without any unified manufacturing standard. In addition, the forces applied have not even been quantified, which makes findings from difference studies incomparable. Moreover, the specific mechanisms behind the positive phenomena of electromagnetic field stimulation in enthesis regeneration have not been fully determined. In future, the most appropriate magnetic field intensity and frequency for enthesis tissue should be tested and specified as early as possible.

In summary, the application of enthesis TE has improved enthesis tissue regeneration. The strategies discussed in this review are expected to promote regeneration of injured enthesis. Moreover, the abundance of the enthesis tissue in vertebra makes it susceptible to damage during avulsion fracture and ankylosing spondylitis. Therefore,

understanding the enthesis TE will benefit research on spine-related enthesis TE.

### Author contributions

Wangwang Luo: Writing-original draft. Yang Wang: Conceptualization. Qin Han: Revised, Supervision. Zhonghan Wang: Supervision. Jianhang Jiao: Literature collection. Xuqiang Gong: Supervision. Yang Liu: Investigation. Aobo Zhang: Investigation. Han Zhang: Literature collection. Hao Chen: Supervision, Methodology. Jincheng Wang: Supervision, Methodology. Minfei Wu: Investigation, Methodology, Funding support.

### Declaration of conflicting interests

The author(s) declared no potential conflicts of interest with respect to the research, authorship, and/or publication of this article.

### Funding

The author(s) disclosed receipt of the following financial support for the research, authorship, and/or publication of this article: This study was supported by

- (1) National Natural Science Foundation of China [grant numbers 82272504, 82072456]
- (2) National Key R&D Program of China [No. 2018YFB1105100]
- (3) Department of Science and Technology of Jilin Province, P.R.C [grant numbers YDZJ202201ZYTS131, YDZJ202201ZYTS129, 202201ZYTS505, 20220204119YY, 20220401084YY, 20210101321JC, 20210204104YY, 20200201448JC, 20200404202YY, 20200403086SF, 20200201453JC]
- (4) Department of Finance in Jilin province [grant number 2020SCZT037, 2019SCZT031]
- (5) Jilin Province Development and Reform Commission, P.R.C [grant numbers 2018C010 & 2022C043-5]
- (6) Interdisciplinary Integration and Cultivation Project of Jilin University [grant number JLUXKJC2020307]

### ORCID iD

Minfei Wu  <https://orcid.org/0000-0001-9736-6778>

### References

1. Thomopoulos S, Williams GR, Gimbel JA, et al. Variation of biomechanical, structural, and compositional properties along the tendon to bone insertion site. *J Orthop Res* 2003; 21: 413–419.
2. Wang IE, Mitroo S, Chen FH, et al. Age-dependent changes in matrix composition and organization at the ligament-to-bone insertion. *J Orthop Res* 2006; 24: 1745–1755.
3. Brown ME and Puetzer JL. Driving native-like zonal enthesis formation in engineered ligaments using mechanical boundary conditions and  $\beta$ -tricalcium phosphate. *Acta Biomater* 2022; 140: 700–716.
4. Roffino S, Camy C, Foucault-Bertaud A, et al. Negative impact of disuse and unloading on tendon enthesis structure and function. *Life Sci Space Res* 2021; 29: 46–52.
5. Sanders TL, Maradit Kremers H, Bryan AJ, et al. Incidence of anterior cruciate ligament tears and reconstruction: a 21-year population-based study. *Am J Sports Med* 2016; 44: 1502–1507.

6. Faruch Bilfeld M, Cavaignac E, Wytrykowski K, et al. Anterolateral ligament injuries in knees with an anterior cruciate ligament tear: contribution of ultrasonography and MRI. *Eur Radiol* 2018; 28: 58–65.
7. Fernández-Sueiro JL. Enthesis as a target element in spondylarthritides. *Reumatol Clin* 2006; 2: 31–35.
8. Abbah SA, Spanoudes K, O'Brien T, et al. Assessment of stem cell carriers for tendon tissue engineering in pre-clinical models. *Stem Cell Res Ther* 2014; 5: 38.
9. Lomas AJ, Ryan CN, Sorushanova A, et al. The past, present and future in scaffold-based tendon treatments. *Adv Drug Deliv Rev* 2015; 84: 257–277.
10. Lee-Barthel A, Lee CA, Vidal MA, et al. Localized BMP-4 release improves the entheses of engineered bone-to-bone ligaments. *Transl Sports Med* 2018; 1: 60–72.
11. Chen C and Hunt KJ. Open reconstructive strategies for Chronic Achilles tendon ruptures. *Foot Ankle Clin* 2019; 24: 425–437.
12. Metso L, Bister V, Sandelin J, et al. A prospective comparison of 3 hamstring ACL fixation devices—rigidfix, bioscrew, and intrafix—randomized into 4 groups with a minimum follow-up of 5 years. *BMC Surg* 2022; 22: 254.
13. Ovigüe J, Graveléau N and Bouguennec N. Patellar tendon reconstruction using hamstring tendon and adjustable suspensory cortical fixation. *Arthrosc Tech* 2019; 8: E679–E683.
14. Xavier PM, Fournier J, de Courtivron B, et al. Rare ACL entheses tears treated by suture in children. a report of 14 cases after a mean 15 years follow-up. *OrthopTraumatol-Surg Res* 2016; 102: 619–623.
15. Schanda JE, Obermayer-Pietsch B, Sommer G, et al. Biomechanical properties of a suture anchor system from human allogenic mineralized cortical bone matrix for rotator cuff repair. *BMC Musculoskelet Disord* 2022; 23: 422.
16. Bagir M, Mirioglu A, Kundakci B, et al. Relationship between the suture materials used in extensor tendon injuries and reoperations. *Cukurova Med J* 2021; 46: 1394–1400.
17. Fletcher D, Sirch FJ, Fletcher C, et al. Failure of the interference tenodesis screw after distal bicep tendon repair with a suture button technique: a report of two cases. *Cureus* 2021; 13: e13779.
18. Karahasanoğlu İ. Biomechanical examination of patellar tendon ruptures repaired with a tendon graft: an experimental study. *Eklem Hastalıkları Ve Cerrahisi-It Dis Relat Surg* 2014; 25: 47–51.
19. Mousavi SH, Masoumi O, Akbariaghdam H, et al. Investigation of hamstring tendon graft fixation for the reconstruction of anterior cruciate ligament using interference screw merely or in combination with supplementary staple: a clinical trial. *Adv Biomed Res* 2020; 9: 52.
20. Wang B, Liu H, Hou W, et al. Biomechanical analysis of bilateral facet joint stabilization for posterior cervical spine reconstruction with bio-derived tendon in goats. *Chin J Reparative Reconstr Surg* 2012; 26: 396–400.
21. Monda MK, Ellis A and Karmani S. Late rupture of flexor pollicis longus tendon 10 years after volar buttress plate fixation of a distal radius fracture: a case report. *Acta Orthop Belg* 2010; 76: 549–551.
22. Quach T, Jazayeri R, Sherman OH, et al. Distal biceps tendon injuries—current treatment options. *Bull NYU Hosp Jt Dis* 2010; 68: 103–111.
23. Dunphy TR, Hudson J, Batech M, et al. Surgical treatment of distal biceps tendon ruptures: an analysis of complications in 784 surgical repairs. *Am J Sports Med* 2017; 45: 3020–3029.
24. Smith L, Xia Y, Galatz LM, et al. Tissue-engineering strategies for the tendon/ligament-to-bone insertion. *Connect Tissue Res* 2012; 53: 95–105.
25. Lu HH and Thomopoulos S. Functional attachment of soft tissues to bone: development, healing, and tissue engineering. *Annu Rev Biomed Eng* 2013; 15: 201–226.
26. Berntsen L, Forghani A and Hayes DJ. Mesenchymal stem cell sheets for engineering of the tendon-bone Interface. *Tissue Eng Part A* 2022; 28: 341–352.
27. Chen H, Li S, Xiao H, et al. Effect of exercise intensity on the healing of the bone-tendon interface: a mouse rotator cuff injury model study. *Am J Sports Med* 2021; 49: 2064–2073.
28. He SK, Ning LJ, Yao X, et al. Hierarchically demineralized cortical bone combined with stem cell-derived extracellular matrix for regeneration of the tendon-bone interface. *Am J Sports Med* 2021; 49: 1323–1332.
29. Olvera D, Sathy BN and Kelly DJ. Spatial presentation of tissue-specific extracellular matrix components along electrospun scaffolds for tissue engineering the bone–ligament interface. *ACS Biomater Sci Eng* 2020; 6: 5145–5161.
30. Tarafder S, Brito JA, Minhas S, et al. *In situ* tissue engineering of the tendon-to-bone interface by endogenous stem/progenitor cells. *Biofabrication* 2019; 12: 015008.
31. Song W, Ma Z, Wang C, et al. Pro-chondrogenic and immunomodulatory melatonin-loaded electrospun membranes for tendon-to-bone healing. *J Mater Chem B* 2019; 7: 6564–6575.
32. Liu Q, Hatta T, Qi J, et al. Novel engineered tendon-fibrocartilage-bone composite with cyclic tension for rotator cuff repair. *J Regen Med Tissue Eng* 2018; 12: 1690–1701.
33. Harada Y, Mifune Y, Inui A, et al. Rotator cuff repair using cell sheets derived from human rotator cuff in a rat model. *J Orthop Res* 2017; 35: 289–296.
34. Hurley-Novatny A, Arumugasamy N, Kimicata M, et al. Concurrent multi-lineage differentiation of mesenchymal stem cells through spatial presentation of growth factors. *Biomed Mater* 2020; 15: 055035.
35. El Jamal A, Briolay A, Mebarek S, et al. Cytokine-induced and stretch-induced sphingosine 1-Phosphate production by entheses cells could favor abnormal ossification in spondyloarthritis. *J Bone Miner Res* 2019; 34: 2264–2276.
36. Elnikety S, Pendegrass CJ, de Godoy RF, et al. Augmentation and repair of tendons using demineralised cortical bone. *BMC Musculoskelet Disord* 2016; 17: 483.
37. Sundar S, Pendegrass CJ, Oddy MJ, et al. Tendon re-attachment to metal prostheses in an in vivo animal model using demineralised bone matrix. *J Bone Joint Surg-Br* 2009; 91B: 1257–1262.
38. Cong S, Sun Y, Lin J, et al. A synthetic graft with multilayered co-electrospinning nanoscaffolds for bridging massive rotator cuff tear in a rat model. *Am J Sports Med* 2020; 48: 1826–1836.

39. Chen C, Chen Y, Li M, et al. Functional decellularized fibrocartilaginous matrix graft for rotator cuff enthesis regeneration: a novel technique to avoid in-vitro loading of cells. *Biomaterials* 2020; 250: 119996.
40. Kovacevic D, Suriani RJ, Jr., Levine WN, et al. Augmentation of rotator cuff healing with Orthobiologics. *J Am Acad Orthop Surg* 2022; 30: e508–e516.
41. Castro AA, Karakostis FA, Copes LE, et al. Effects of selective breeding for voluntary exercise, chronic exercise, and their interaction on muscle attachment site morphology in house mice. *J Anat* 2022; 240: 279–295.
42. Romeo A, Easley J, Regan D, et al. Rotator cuff repair using a bioresorbable nanofiber interposition scaffold: a biomechanical and histologic analysis in sheep. *J Shoulder Elbow Surg* 2022; 31: 402–412.
43. Yu SM and Yu JS. Calcaneal avulsion fractures: an often forgotten diagnosis. *Am J Roentgenol* 2015; 205: 1061–1067.
44. Calpur O, Copuroglu C and Ozcan M. Avulsion fractures of both anterior and posterior cruciate ligament tibial insertions. *Knee Surg Sports Traumatol Arthrosc* 2002; 10: 223–225.
45. Scholten R and Boons HW. Complete avulsion of the rotator cuff footprint in an irreducible traumatic posterior glenohumeral fracture-dislocation due to infraspinatus interposition. *J Shoulder Elbow Surg* 2017; 26: E259–E263.
46. Zumstein MA, Lädermann A, Raniga S, et al. The biology of rotator cuff healing. *Orthop Traumatol-Surg Res* 2017; 103: S1–S10.
47. Reese SP, Maas SA and Weiss JA. Micromechanical models of helical superstructures in ligament and tendon fibers predict large Poisson's ratios. *J Biomech* 2010; 43: 1394–1400.
48. Gautieri A, Vesentini S, Redaelli A, et al. Hierarchical structure and nanomechanics of collagen microfibrils from the atomistic scale up. *Nano Lett* 2011; 11: 757–766.
49. Kannus P. Structure of the tendon connective tissue. *Scand J Med Sci Sports* 2000; 10: 312–320.
50. Kastelic J, Galeski A and Baer E. The multicomposite structure of tendon. *Connect Tissue Res* 1978; 6: 11–23.
51. Fallon J, Blevins FT, Vogel K, et al. Functional morphology of the supraspinatus tendon. *J Orthop Res* 2002; 20: 920–926.
52. Hess GP, Cappiello WL, Poole RM, et al. Prevention and treatment of overuse tendon injuries. *Sports Med* 1989; 8: 371–384.
53. Karimi H, Seyed-Foroootan K and Karimi A-M. Stem cells and tendon regeneration. In: Duscher D and Shiffman MA (eds) *Regenerative medicine and plastic surgery: skin and soft tissue, bone, cartilage, muscle, tendon and nerves*. Cham: Springer International Publishing, 2019, pp.369–384.
54. Tencone F, Della Villa S and Giannini A. Conservative treatments for tendinopathy. In: Canata GL, d'Hooghe P and Hunt KJ (eds) *Muscle and tendon injuries: evaluation and management*. Berlin, Heidelberg: Springer, 2017, pp.157–174.
55. Tang JB. Tendon injuries across the world: treatment. *Injury* 2006; 37: 1036–1042.
56. Birk DE and Zycband E. Assembly of the tendon extracellular matrix during development. *J Anat* 1994; 184 (Pt 3): 457–463.
57. Strocchi R, De Pasquale V, Guizzardi S, et al. Human Achilles tendon: morphological and morphometric variations as a function of age. *Foot Ankle* 1991; 12: 100–104.
58. Beck K and Brodsky B. Supercoiled protein motifs: the collagen triple-helix and the alpha-helical coiled coil. *J Struct Biol* 1998; 122: 17–29.
59. Rufai A, Ralphs JR and Benjamin M. Ultrastructure of fibrocartilages at the insertion of the rat Achilles tendon. *J Anat* 1996; 189 (Pt 1): 185–191.
60. Ralphs JR, Benjamin M and Thornett A. Cell and matrix biology of the suprapatella in the rat: a structural and immunocytochemical study of fibrocartilage in a tendon subject to compression. *Anat Rec* 1991; 231: 167–177.
61. Niyibizi C, Sagarrigo Visconti C, Gibson G, et al. Identification and immunolocalization of type X collagen at the ligament-bone interface. *Biochem Biophys Res Commun* 1996; 222: 584–589.
62. Waggett AD, Ralphs JR, Kwan AP, et al. Characterization of collagens and proteoglycans at the insertion of the human Achilles tendon. *Matrix Biol* 1998; 16: 457–470.
63. Yoon JH and Halper J. Tendon proteoglycans: biochemistry and function. *J Musculoskelet Neuronal Interact* 2005; 5: 22–34.
64. Corps AN, Robinson AH, Movin T, et al. Versican splice variant messenger RNA expression in normal human Achilles tendon and tendinopathies. *Rheumatology* 2004; 43: 969–972.
65. Mansson B, Wenglén C, Mörgelin M, et al. Association of chondroadherin with collagen type II. *J Biol Chem* 2001; 276: 32883–32888.
66. Corps AN, Robinson AH, Movin T, et al. Increased expression of aggrecan and biglycan mRNA in Achilles tendinopathy. *Rheumatology* 2006; 45: 291–294.
67. Wiberg C, Klatt AR, Wagener R, et al. Complexes of matrilin-1 and biglycan or decorin connect collagen VI microfibrils to both collagen II and aggrecan. *J Biol Chem* 2003; 278: 37698–37704.
68. Rigozzi S, Müller R, Stemmer A, et al. Tendon glycosaminoglycan proteoglycan sidechains promote collagen fibril sliding-AFM observations at the nanoscale. *J Biomech* 2013; 46: 813–818.
69. Ralphs JR, Benjamin M, Waggett AD, et al. Regional differences in cell shape and gap junction expression in rat Achilles tendon: relation to fibrocartilage differentiation. *J Anat* 1998; 193 ( Pt 2): 215–222.
70. Boonrungsiman S, Gentleman E, Carzaniga R, et al. The role of intracellular calcium phosphate in osteoblast-mediated bone apatite formation. *Proc Natl Acad Sci U S A* 2012; 109: 14170–14175.
71. Shao C, Zhao R, Jiang S, et al. Citrate improves collagen mineralization via interface wetting: A physicochemical understanding of biomineralization control. *Adv Mater Weinheim* 2018; 30: eng98853580935–eng98896481521.
72. Sinclair KD, Curtis BD, Koller KE, et al. Characterization of the anchoring morphology and mineral content of the anterior cruciate and medial collateral ligaments of the knee. *Anat Rec-Adv Integr Anat Evol Biol* 2011; 294: 831–838.
73. Buenzli PR and Sims NA. Quantifying the osteocyte network in the human skeleton. *Bone* 2015; 75: 144–150.



74. Spalazzi JP, Boskey AL, Pleshko N, et al. Quantitative mapping of matrix content and distribution across the ligament-to-bone insertion. *PLoS One* 2013; 8: e74349.
75. Kajave NS, Schmitt T, Patrawalla NY, et al. Design-build-validate strategy to 3D print bioglass gradients for anterior cruciate ligament enthesis reconstruction. *Tissue Eng Part C Methods* 2022; 28: 158–167.
76. Matyas JR, Anton MG, Shrive NG, et al. Stress governs tissue phenotype at the femoral insertion of the rabbit MCL. *J Biomech* 1995; 28: 147–157.
77. Benjamin M and Ralphs JR. Fibrocartilage in tendons and ligaments—an adaptation to compressive load. *J Anat* 1998; 193 (Pt 4): 481–494.
78. Spalazzi JP, Gallina J, Fung-Kee-Fung SD, et al. Elastographic imaging of strain distribution in the anterior cruciate ligament and at the ligament-bone insertions. *J Orthop Res* 2006; 24: 2001–2010.
79. Moffat KL, Sun WH, Pena PE, et al. Characterization of the structure-function relationship at the ligament-to-bone interface. *Proc Natl Acad Sci U S A* 2008; 105: 7947–7952.
80. Leong NL, Kator JL, Clemens TL, et al. Tendon and ligament healing and current approaches to tendon and ligament regeneration. *J Orthop Res* 2020; 38: 7–12.
81. Weiler A, Hoffmann RFG, Bail HJ, et al. Tendon healing in a bone tunnel. Part II: histologic analysis after biodegradable interference fit fixation in a model of anterior cruciate ligament reconstruction in sheep. *Arthrosc J Arthrosc Relat Surg* 2002; 18: 124–135.
82. Tabuchi K, Soejima T, Kanazawa T, et al. Chronological changes in the collagen-type composition at tendon–bone interface in rabbits. *Bone Jt Res* 2012; 1: 218–224.
83. Terzi A, Gallo N, Bettini S, et al. Sub- and supramolecular X-Ray characterization of engineered tissues from equine tendon, bovine dermis, and fish skin type-I collagen. *Macromol Biosci* 2020; 20: e2000017.
84. Chaplin DM. The vascular anatomy within normal tendons, divided tendons, free tendon grafts and pedicle tendon grafts in Rabbits. *J Bone Joint Surg Br* 1973; 55-B: 369–389.
85. Ciatti R and Mariani PP. Fibroma of tendon sheath located within the ankle joint capsule. *J Orthop Traumatol* 2009; 10: 147–150.
86. Koob TJ and Summers AP. Tendon—bridging the gap. *Comp Biochem Physiol A-Mol and Integr Physiol* 2002; 133: 905–909.
87. Garner WL, McDonald JA, Koo M, et al. Identification of the collagen-producing cells in healing flexor tendons. *Plast Reconstr Surg* 1989; 83: 875–879.
88. Wang ED. Tendon repair. *J Hand Ther* 1998; 11: 105–110.
89. Loisel AE, Frisch BJ, Wolenski M, et al. Bone marrow-derived matrix metalloproteinase-9 is associated with fibrous adhesion formation after murine flexor tendon injury. *PLoS One* 2012; 7: e40602.
90. Tang C, Chen Y, Huang J, et al. The roles of inflammatory mediators and immunocytes in tendinopathy. *J Orthop Translat* 2018; 14: 23–33.
91. Nichols AE, Best KT and Loisel AE. The cellular basis of fibrotic tendon healing: challenges and opportunities. *Transl Res* 2019; 209: 156–168.
92. Gotoh M, Hamada K, Yamakawa H, et al. Significance of granulation tissue in torn supraspinatus insertions: an immunohistochemical study with antibodies against interleukin-1 beta, cathepsin D, and matrix metalloprotease-1. *J Orthop Res Off Publ Orthop Res Soc* 1997; 15: 33–39.
93. Abrams GD, Luria A, Carr RA, et al. Association of synovial inflammation and inflammatory mediators with glenohumeral rotator cuff pathology. *J Shoulder Elbow Surg* 2016; 25: 989–997.
94. Schneider M, Angele P, Järvinen TAH, et al. Rescue plan for Achilles: therapeutics steering the fate and functions of stem cells in tendon wound healing. *Adv Drug Deliv Rev* 2018; 129: 352–375.
95. Ho JO, Sawadkar P and Mudera V. A review on the use of cell therapy in the treatment of tendon disease and injuries. *J Tissue Eng* 2014; 5: 2041731414549678.
96. Ruiz-Alonso S, Lafuente-Merchan M, Ciriza J, et al. Tendon tissue engineering: cells, growth factors, scaffolds and production techniques. *J Control Release* 2021; 333: 448–486.
97. Rathbun JB and Macnab I. The microvascular pattern of the rotator cuff. *J Bone Jt Surg Br vol* 1970; 52-B: 540–553.
98. Sharma P and Maffulli N. Biology of tendon injury: healing, modeling and remodeling. *J Musculoskelet Neuronal Interact* 2006; 6: 181–190.
99. Docheva D, Müller SA, Majewski M, et al. Biologics for tendon repair. *Adv Drug Deliv Rev* 2015; 84: 222–239.
100. Howell K, Chien C, Bell R, et al. Novel model of tendon regeneration reveals distinct cell mechanisms underlying regenerative and fibrotic tendon healing. *Sci Rep* 2017; 7: 45238.
101. Beredjikian PK, Favata M, Cartmell JS, et al. Regenerative versus reparative healing in tendon: A study of biomechanical and histological properties in fetal sheep. *Ann Biomed Eng* 2003; 31: 1143–1152.
102. Tang QM, Chen JL, Shen WL, et al. Fetal and adult fibroblasts display intrinsic differences in tendon tissue engineering and regeneration. *Sci Rep* 2014; 4: 5515.
103. Xu Q, Sun WX and Zhang ZF. High expression of VEGFA in MSCs promotes tendon-bone healing of rotator cuff tear via microRNA-205-5p. *Eur Rev Med Pharmacol Sci* 2019; 23: 4081–4088.
104. Uz U, Gunhan K, Vatansver S, et al. Novel simple strategy for cartilage tissue engineering using stem cells and synthetic polymer scaffold. *J Craniofac Surg* 2019; 30: 940–943.
105. Huang Y, Pan M, Shu H, et al. Vascular endothelial growth factor enhances tendon-bone healing by activating yes-associated protein for angiogenesis induction and rotator cuff reconstruction in rats. *J Cell Biochem* 2020; 121: 2343–2353.
106. Rodríguez-Vázquez M and Ramos-Zúñiga R. Chitosan-hydroxyapatite scaffold for tissue engineering in experimental lumbar laminectomy and posterolateral spinal fusion in Wistar Rats. *Asian Spine J* 2020; 14: 139–147.
107. Sadeghinia A, Soltani S, Aghazadeh M, et al. Design and fabrication of clinoptilolite–nanohydroxyapatite/chitosan–gelatin composite scaffold and evaluation of its effects on bone tissue engineering. *J Biomed Mater Res A* 2020; 108: 221–233.
108. Langer R and Vacanti JP. Tissue engineering. *Science* 1993; 260: 920–926.

109. Sharma P, Kumar P, Sharma R, et al. Tissue Engineering; current status & Futuristic scope. *J M Life* 2019; 12: 225–229.
110. Sangkert S, Kamolmatyakul S and Meesane J. The bone-mimicking effect of calcium phosphate on composite chitosan scaffolds in maxillofacial bone tissue engineering. *J Appl Biomater Funct Mater* 2020; 18: 1–8. DOI: 10.1177/2280800019893204
111. Zeng S, Ye J, Cui Z, et al. Surface biofunctionalization of three-dimensional porous poly(lactic acid) scaffold using chitosan/OGP coating for bone tissue engineering. *Mater Sci Eng C-Mater Biol Appl* 2017; 77: 92–101.
112. Jaidev LR and Chatterjee K. Surface functionalization of 3D printed polymer scaffolds to augment stem cell response. *Mater Des* 2019; 161: 44–54.
113. Chen C, Zhu J, Chen J, et al. A reinforced nanofibrous patch with biomimetic mechanical properties and chondroinductive effect for rotator cuff tissue engineering. *Mater Today Chem* 2022; 23: 1–15. DOI: 10.1016/j.mtchem.2021.100655
114. Chen P, Wang S, Huang Z, et al. Multi-functionalized nanofibers with reactive oxygen species scavenging capability and fibrocartilage inductivity for tendon-bone integration. *J Mater Sci Technol* 2021; 70: 91–104.
115. Gottardi R, Moeller K, Di Gesù R, et al. Application of a hyperelastic 3D printed scaffold for mesenchymal stem cell-based fabrication of a bizonal tendon enthesis-like construct. *Front Mater* 2021; 8: 1–9. DOI: 10.3389/fmats.2021.613212
116. Peniche Silva CJ, Müller SA, Quirk N, et al. Enthesis healing is dependent on scaffold interphase morphology—results from a rodent patellar model. *Cells* 2022; 11: eng1016000522073.
117. Sensini A, Massafra G, Gotti C, et al. Tissue engineering for the insertions of tendons and ligaments: an overview of electrospun biomaterials and structures. *Front Bioeng Biotechnol* 2021; 9: 645544.
118. Su W, Guo J, Xu J, et al. Gradient composite film with calcium phosphate silicate for improved tendon -to-bone intergration. *Chem Eng J* 2021; 404: 1–12. DOI: 10.1016/j.cej.2020.126473
119. Atesok K, Doral MN, Karlsson J, et al. Multilayer scaffolds in orthopaedic tissue engineering. *Knee Surg Sports Traumatol Arthrosc* 2016; 24: 2365–2373.
120. Criscenti G, Longoni A, Di Luca A, et al. Triphasic scaffolds for the regeneration of the bone-ligament interface. *Biofabrication* 2016; 8: 015009.
121. Li X, Xie J, Lipner J, et al. Nanofiber scaffolds with gradations in mineral content for mimicking the tendon-to-bone insertion site. *Nano Lett* 2009; 9: 2763–2768.
122. Liu W, Lipner J, Xie J, et al. Nanofiber scaffolds with gradients in mineral content for spatial control of osteogenesis. *ACS Appl Mater Interfaces* 2014; 6: 2842–2849.
123. Samavedi S, Olsen Horton C, Guelcher SA, et al. Fabrication of a model continuously graded co-electrospun mesh for regeneration of the ligament–bone interface. *Acta Biomater* 2011; 7: 4131–4138.
124. Samavedi S, Guelcher SA, Goldstein AS, et al. Response of bone marrow stromal cells to graded co-electrospun scaffolds and its implications for engineering the ligament-bone interface. *Biomaterials* 2012; 33: 7727–7735.
125. Ramalingam M, Young MF, Thomas V, et al. Nanofiber scaffold gradients for interfacial tissue engineering. *J Biomater Appl* 2013; 27: 695–705.
126. Calejo I, Costa-Almeida R, Reis RL, et al. A textile platform using continuous aligned and textured composite microfibers to engineer tendon-to-bone interface gradient scaffolds. *Adv Healthc Mater* 2019; 8: e1900200.
127. Zhu C, Pongkitwitoon S, Qiu J, et al. Design and fabrication of a hierarchically structured scaffold for tendon-to-bone repair. *Adv Mater.* 2018; 30: e1707306.
128. Liu GM, Pan J, Zhang Y, et al. Bridging repair of large rotator cuff tears using a multilayer decellularized tendon slices graft in a rabbit model. *Arthrosc J Arthrosc Relat Surg* 2018; 34: 2569–2578.
129. Lan T, Chen J, Zhang J, et al. Xenoextracellular matrix-rosiglitazone complex-mediated immune evasion promotes xenogenic bioengineered root regeneration by altering M1/M2 macrophage polarization. *Biomaterials* 2021; 276: 121066.
130. Chen C, Shi Q, Li M, et al. Engineering an enthesis-like graft for rotator cuff repair: an approach to fabricate highly biomimetic scaffold capable of zone-specifically releasing stem cell differentiation inducers. *Bioact Mater* 2022; 16: 451–471.
131. Zuo R, Liu J, Zhang Y, et al. In situ regeneration of bone-to-tendon structures: comparisons between costal-cartilage derived stem cells and BMSCs in the rat model. *Acta Biomater* 2022; 145: 62–76.
132. Shengnan Q, Bennett S, Wen W, et al. The role of tendon derived stem/progenitor cells and extracellular matrix components in the bone tendon junction repair. *Bone* 2021; 153: 116172.
133. Xu K, Kuntz LA, Foehr P, et al. Efficient decellularization for tissue engineering of the tendon-bone interface with preservation of biomechanics. *PLoS One* 2017; 12: e0171577.
134. Su M, Zhang Q, Zhu Y, et al. Preparation of decellularized triphasic hierarchical bone-fibrocartilage-tendon composite extracellular matrix for enthesis regeneration. *Adv Healthc Mater* 2019; 8: e1900831.
135. Shi Q, Chen C, Li M, et al. Characterization of the distributions of collagen and PGs content in the decellularized book-shaped enthesis scaffolds by SR-FTIR. *BMC Musculoskelet Disord* 2021; 22: 235.
136. Shi Q, Chen Y, Li M, et al. Designing a novel vacuum aspiration system to decellularize large-size enthesis with preservation of physicochemical and biological properties. *Ann Transl Med* 2020; 8: 1364–1364.
137. Mao Z, Fan B, Wang X, et al. A systematic review of tissue engineering scaffold in tendon bone healing in vivo. *Front Bioeng Biotechnol* 2021; 9: 621483.
138. Lin Z, Tao Y, Huang Y, et al. Applications of marine collagens in bone tissue engineering. *Biomed Mater* 2021; 16: 042007.
139. Quan T and Fisher GJ. Role of age-associated alterations of the dermal extracellular matrix microenvironment in human skin aging: A mini-review. *Gerontology* 2015; 61: 427–434.

140. Kim H, Jang J, Park J, et al. Shear-induced alignment of collagen fibrils using 3D cell printing for corneal stroma tissue engineering. *Biofabrication* 2019; 11: 035017.
141. Shi Y, H elary C and Coradin T. Exploring the cell-protein-mineral interfaces: Interplay of silica (nano)rods@collagen biocomposites with human dermal fibroblasts. *Mater Today Bio* 2019; 1: 100004.
142. Mohammed D, Pardon G, Versaevel M, et al. Producing collagen micro-stripes with aligned fibers for cell migration assays. *Cell Mol Bioeng* 2020; 13: 87–98.
143. Sharma V, Kumar A, Puri K, et al. Application of platelet-rich fibrin membrane and collagen dressing as palatal bandage for wound healing: A randomized clinical control trial. *Ind J Dent Res* 2019; 30: 881–888.
144. Tonndorf R, Aibibu D and Cherif C. Collagen multifilament spinning. *Mater Sci Eng C-Mater Biol Appl* 2020; 106: 110105.
145. Young RG, Butler DL, Weber W, et al. Use of mesenchymal stem cells in a collagen matrix for Achilles tendon repair. *J Orthop Res* 1998; 16: 406–413.
146. Fleming BC, Spindler KP, Palmer MP, et al. Collagen-platelet composites improve the biomechanical properties of healing anterior cruciate ligament grafts in a porcine model. *Am J Sports Med* 2009; 37: 1554–1563.
147. Bi F, Shi Z, Liu A, et al. Anterior cruciate ligament reconstruction in a rabbit model using silk-collagen scaffold and comparison with autograft. *PLoS One* 2015; 10: e0125900.
148. Kovacevic D, Gulotta LV, Ying L, et al. rhPDGF-BB promotes early healing in a rat rotator cuff repair model. *Clin Orthop Relat Res* 2015; 473: 1644–1654.
149. Learn GD, McClellan PE, Knapik DM, et al. Woven collagen biotextiles enable mechanically functional rotator cuff tendon regeneration during repair of segmental tendon defects in vivo. *J Biomed Mater Res B-Appl Biomater* 2019; 107: 1864–1876.
150. Zhu M, Tay ML, Callon K, et al. Overlay repair with a synthetic collagen scaffold improves the quality of healing in a rat rotator cuff repair model. *J Shoulder Elbow Surg* 2019; 28: 949–958.
151. Torres DS, Freyman TM, Yannas IV, et al. Tendon cell contraction of collagen-GAG matrices in vitro: effect of cross-linking. *Biomaterials* 2000; 21: 1607–1619.
152. Ro bach BP, G ulecy z MF, Kempfert L, et al. Rotator cuff repair with autologous tenocytes and biodegradable collagen scaffold: A histological and biomechanical study in sheep. *Am J Sports Med* 2020; 48: 450–459.
153. Awad HA, Boivin GP, Dressler MR, et al. Repair of patellar tendon injuries using a cell-collagen composite. *J Orthop Res* 2003; 21: 420–431.
154. Rieu C, Picaut L, Mosser G, et al. From tendon injury to collagen-based tendon regeneration: Overview and recent advances. *Curr Pharm Des* 2017; 23: 3483–3506.
155. Yang S, Shi X, Li X, et al. Oriented collagen fiber membranes formed through counter-rotating extrusion and their application in tendon regeneration. *Biomaterials* 2019; 207: 61–75.
156. Lin Y, Zhang L, Liu NQ, et al. In vitro behavior of tendon stem/progenitor cells on bioactive electrospun nanofiber membranes for tendon-bone tissue engineering applications. *Int J Nanomedicine* 2019; 14: 5831–5848.
157. Brougham CM, Levingstone TJ, Shen N, et al. Freeze-drying as a novel biofabrication method for achieving a controlled microarchitecture within large, complex natural biomaterial scaffolds. *Adv Healthc Mater* 2017; 6: eng1015816132192.
158. Pogorelov AG and Selezneva II. Evaluation of collagen gel microstructure by scanning electron microscopy. *Bull Exp Biol Med* 2010; 150: 153–156.
159. Haugh MG, Murphy CM and O’Brien FJ. Novel Freeze-drying methods to produce a range of collagen-glycosaminoglycan scaffolds with tailored mean pore sizes. *Tissue Eng Part C-Methods* 2010; 16: 887–894.
160. Caliar SR, Weisgerber DW, Grier WK, et al. Collagen scaffolds incorporating coincident gradations of instructive structural and biochemical cues for osteotendinous junction engineering. *Adv Healthc Mater* 2015; 4: 831–837.
161. Sun Han Chang RA, Shanley JF, Kersh ME, et al. Tough and tunable scaffold-hydrogel composite biomaterial for soft-to-hard musculoskeletal tissue interfaces. *Sci Adv* 2020; 6: eabb6763.
162. Younesi M, Islam A, Kishore V, et al. Tenogenic induction of human MSCs by anisotropically aligned collagen biotextiles. *Adv Funct Mater* 2014; 24: 5762–5770.
163. Cheng X, Gurkan UA, Dehen CJ, et al. An electrochemical fabrication process for the assembly of anisotropically oriented collagen bundles. *Biomaterials* 2008; 29: 3278–3288.
164. Kishore V, Bullock W, Sun X, et al. Tenogenic differentiation of human MSCs induced by the topography of electrochemically aligned collagen threads. *Biomaterials* 2012; 33: 2137–2144.
165. Younesi M, Goldberg VM and Akkus O. A micro-architecturally biomimetic collagen template for mesenchymal condensation based cartilage regeneration. *Acta Biomater* 2016; 30: 212–221.
166. Bose S, Li S, Mele E, et al. Exploring the mechanical properties and performance of Type-I collagen at various length scales: a progress report. *Materials* 2022; 15: 2753.
167. Zhu B, Li W, Chi N, et al. Optimization of glutaraldehyde vapor treatment for electrospun collagen/silk tissue engineering scaffolds. *ACS Omega* 2017; 2: 2439–2450.
168. Sionkowska A and Kozłowska J. Properties and modification of porous 3-D collagen/hydroxyapatite composites. *Int J Biol Macromol* 2013; 52: 250–259.
169. Delgado LM, Fuller K and Zeugolis DI. Collagen cross-linking: biophysical, biochemical, and biological response analysis. *Tissue Eng Part A* 2017; 23: 1064–1077.
170. Pissarenko A, Yang W, Quan H, et al. Tensile behavior and structural characterization of pig dermis. *Acta Biomater* 2019; 86: 77–95.
171. Huang CC. Design and characterization of a bioinspired polyvinyl alcohol matrix with structural foam-wall microarchitectures for potential tissue engineering applications. *Polymers* 2022; 14: eng1015453572073.
172. Andriotis OG, Manuyakorn W, Zekonyte J, et al. Nano-mechanical assessment of human and murine collagen fibrils via atomic force microscopy cantilever-based nanoindentation. *J Mech Behav Biomed Mater* 2014; 39: 9–26.

173. Kim SH, Park HS, Lee OJ, et al. Fabrication of duck's feet collagen-silk hybrid biomaterial for tissue engineering. *Int J Biol Macromol* 2016; 85: 442–450.
174. Ahn S, Lee S, Cho Y, et al. Fabrication of three-dimensional collagen scaffold using an inverse mould-leaching process. *Bioprocess Biosyst Eng* 2011; 34: 903–911.
175. El Blidi O, El Omari N, Balahbib A, et al. Extraction methods, characterization and biomedical applications of collagen: a review. *Biointerface Res Appl Chem* 2021; 11: 13587–13613.
176. Sanz B, Albillos Sanchez A, Tangey B, et al. Light cross-linkable marine collagen for coaxial printing of a 3D model of neuromuscular junction formation. *Biomedicine* 2020; 9: 16.
177. Gharagheshlagh SN, Fatemi MJ, Jamili S, et al. Isolation and characterization of acid-soluble collagen from the skin of *Rutilus Frisii Kutum* (Kamensky) of the Caspian Sea. *Iran J Fish Sci* 2020; 19: 768–779.
178. Liao S, Murugan R, Chan C, et al. Processing nanoengineered scaffolds through electrospinning and mineralization, suitable for biomimetic bone tissue engineering. *J Mech Behav Biomed Mater* 2008; 1: 252–260.
179. Vieira AC, Guedes RM and Marques AT. Development of ligament tissue biodegradable devices: A review. *J Biomech* 2009; 42: 2421–2430.
180. Ifkovits JL and Burdick JA. Review: Photopolymerizable and degradable biomaterials for tissue engineering applications. *Tissue Eng* 2007; 13: 2369–2385.
181. Parekh N, Bijosh CK, Kane K, et al. Superior processability of *Antheraea mylitta* silk with cryo-milling: performance in bone tissue regeneration. *Int J Biol Macromol* 2022; 213: 155–165.
182. Zhang Q, Bei HP, Zhao M, et al. Shedding light on 3D printing: Printing photo-crosslinkable constructs for tissue engineering. *Biomaterials* 2022; 286: 121566.
183. Shuang FF, Wang CC, Zhu WJ, et al. Preparation of a robust silk fibroin scaffold with a reinforced concrete structure constructed with silk nanofibers as the skeleton based on a CaCl<sub>2</sub>-formic acid solution and freeze-drying method. *Polym Test* 2022; 111: 1–11. DOI: 10.1016/j.polymertesting.2022.107599
184. Hu X, Shmelev K, Sun L, et al. Regulation of silk material structure by temperature-controlled water vapor annealing. *Biomacromolecules* 2011; 12: 1686–1696.
185. Dong X, Zhao Q, Xiao L, et al. Amorphous silk nanofiber solutions for fabricating silk-based functional materials. *Biomacromolecules* 2016; 17: 3000–3006.
186. Han F, Liu S, Liu X, et al. Woven silk fabric-reinforced silk nanofibrous scaffolds for regenerating load-bearing soft tissues. *Acta Biomater* 2014; 10: 921–930.
187. Chen P, Li L, Dong L, et al. Gradient biomimetic silk fibroin nanofibrous scaffold with osteochondral inductivity for integration of tendon to bone. *ACS Biomater Sci Eng* 2021; 7: 841–851.
188. Judawisastra H, Nugraha FR and Wibowo UA. Porous architecture evaluation of silk fibroin scaffold from direct dissolution salt leaching method. In: *International conference on innovation in polymer science and technology (IPST) in conjunction with 7th international conference on fuel cell and hydrogen technology (ICFCHT)*, Indonesian Polymer Assoc, Bali, Indonesia, October 16–19 June 2019. Macromolecular Symposia.
189. Yan LP, Silva-Correia J, Oliveira MB, et al. Bilayered silk/silk-nanoCaP scaffolds for osteochondral tissue engineering: in vitro and in vivo assessment of biological performance. *Acta Biomater* 2015; 12: 227–241.
190. Xiao L, Zhu C, Ding Z, et al. Growth factor-free salt-leached silk scaffolds for differentiating endothelial cells. *J Mater Chem B* 2018; 6: 4308–4313.
191. Ren M, Du C, Herrero Acero E, et al. A biofidelic 3D culture model to study the development of brain cellular systems. *Sci Rep* 2016; 6: 1–15. DOI: 10.1038/srep24953
192. Sánchez-Ortega JF, Vázquez A, Ruiz-Ginés JA, et al. Longitudinal atlantoaxial dislocation associated with type III odontoid fracture due to high-energy trauma. case report and literature review. *Spinal Cord Ser Cases* 2021; 7: 43.
193. Lin PD, Guo X and Ni B. Bilateral atlantoaxial lamina hook and atlantoaxial joint space screw for the treatment of acute type I transverse ligament injury in school-age children. *China J Orthop and Traumatol* 2019; 32: 819–823.
194. Kim UJ, Park J, Kim HJ, et al. Three-dimensional aqueous-derived biomaterial scaffolds from silk fibroin. *Biomaterials* 2005; 26: 2775–2785.
195. Rajkhowa R, Gil ES, Kluge J, et al. Reinforcing silk scaffolds with silk particles. *Macromol Biosci* 2010; 10: 599–611.
196. Sang Y, Li M, Liu J, et al. Biomimetic silk scaffolds with an amorphous structure for soft tissue engineering. *ACS Appl Mater Interfaces* 2018; 10: 9290–9300.
197. Wang Y, Rudym DD, Walsh A, et al. In vivo degradation of three-dimensional silk fibroin scaffolds. *Biomaterials* 2008; 29: 3415–3428.
198. Kasoju N and Bora U. Silk Fibroin in tissue engineering. *Adv Healthc Mater* 2012; 1: 393–412.
199. Altman GH, Diaz F, Jakuba C, et al. Silk-based biomaterials. *Biomaterials* 2003; 24: 401–416.
200. Zarkoob S, Eby RK, Reneker DH, et al. Structure and morphology of electrospun silk nanofibers. *Polymer* 2004; 45: 3973–3977.
201. Gallorini M, Berardi AC, Berardocco M, et al. Hyaluronic acid increases tendon derived cell viability and proliferation in vitro: comparative study of two different hyaluronic acid preparations by molecular weight. *Muscles Ligaments Tendons J* 2017; 7: 208–214.
202. Frizziero A, Salamanna F, Giavaresi G, et al. Hyaluronic acid injections protect patellar tendon from detraining-associated damage. *Histol Histopathol* 2015; 30: 1079–1088.
203. Vindigni V, Tonello C, Lancerotto L, et al. Preliminary report of in vitro reconstruction of a vascularized tendon-like structure a novel application for adipose-derived stem cells. *Ann Plast Surg* 2013; 71: 664–670.
204. Rak Kwon D, Jung S, Jang J, et al. A 3-Dimensional bio-printed scaffold with human umbilical cord blood-mesenchymal stem cells improves regeneration of chronic full-thickness rotator cuff tear in a rabbit model. *Am J Sports Med* 2020; 48: 947–958.
205. Otabe K, Nakahara H, Hasegawa A, et al. Transcription factor Mohawk controls tenogenic differentiation of bone marrow mesenchymal stem cells in vitro and in vivo. *J Orthop Res* 2015; 33(1): 1–8.

206. Han F, Zhang P, Chen T, et al. A LbL-Assembled bioactive coating modified nanofibrous membrane for rapid tendon-bone healing in ACL reconstruction. *Int J Nanomedicine* 2019; 14: 9159–9172.
207. Zhai P, Peng X, Li B, et al. The application of hyaluronic acid in bone regeneration. *Int J Biol Macromol* 2020; 151: 1224–1239.
208. Petrigliano FA, McAllister DR and Wu BM. Tissue engineering for anterior cruciate ligament reconstruction: A review of current strategies. *Arthrosc J Arthrosc Relat Surg* 2006; 22: 441–451.
209. Vunjak-Novakovic G, Altman G, Horan R, et al. Tissue engineering of ligaments. *Annu Rev Biomed Eng* 2004; 6: 131–156.
210. Zuber M, Zia F, Zia KM, et al. Collagen based polyurethanes—A review of recent advances and perspective. *Int J Biol Macromol* 2015; 80: 366–374.
211. Gu R and Sain MM. Effects of wood fiber and microclay on the performance of soy based polyurethane foams. *J Polym Environ* 2013; 21: 30–38.
212. Youssef TE, Al-Turaif H and Wazzan AA. Investigations on the structural and mechanical properties of polyurethane resins based on Cu(II)phthalocyanines. *Int J Polym Sci* 2015; 2015: 1–10.
213. Najafi SJ, Gharehaghaji AA and Etrati SM. Fabrication and characterization of elastic hollow nanofibrous PU yarn. *Mater Des* 2016; 99: 328–334.
214. Yekrang J, Semnani D, Beigi MH, et al. Electrospinning of aligned medical grade polyurethane nanofibres and evaluation of cell–scaffold interaction using SHED stem cells. *Micro Nano Lett* 2017; 12: 412–417.
215. Webb K, Hitchcock RW, Smeal RM, et al. Cyclic strain increases fibroblast proliferation, matrix accumulation, and elastic modulus of fibroblast-seeded polyurethane constructs. *J Biomech* 2006; 39: 1136–1144.
216. Merceron TK, Burt M, Seol YJ, et al. A 3D bioprinted complex structure for engineering the muscle-tendon unit. *Biofabrication* 2015; 7: 035003.
217. Tsai MC, Hung KC, Hung SC, et al. Evaluation of biodegradable elastic scaffolds made of anionic polyurethane for cartilage tissue engineering. *Colloids Surf B Biointerfaces* 2015; 125: 34–44.
218. McBane JE, Sharifpoor S, Cai K, et al. Biodegradation and in vivo biocompatibility of a degradable, polar/hydrophobic/ionic polyurethane for tissue engineering applications. *Biomaterials* 2011; 32: 6034–6044.
219. Shen Z, Guo S, Ye D, et al. Skeletal muscle regeneration on protein-grafted and microchannel-patterned scaffold for hypopharyngeal tissue engineering. *Biomed Res Int* 2013; 2013: 146953.
220. Encalada-Diaz I, Cole BJ, Macgillivray JD, et al. Rotator cuff repair augmentation using a novel polycarbonate polyurethane patch: preliminary results at 12 months' follow-up. *J Shoulder Elbow Surg* 2011; 20: 788–794.
221. Richbourg NR, Peppas NA and Sikavitsas VI. Tuning the biomimetic behavior of scaffolds for regenerative medicine through surface modifications. *J Regen Med Tissue Eng* 2019; 13: 1275–1293.
222. Deng D, Liu W, Xu F, et al. Engineering human neo-tendon tissue in vitro with human dermal fibroblasts under static mechanical strain. *Biomaterials* 2009; 30: 6724–6730.
223. Wang B, Liu W, Zhang Y, et al. Engineering of extensor tendon complex by an ex vivo approach. *Biomaterials* 2008; 29: 2954–2961.
224. Heckmann L, Fiedler J, Mattes T, et al. Interactive effects of growth factors and three-dimensional scaffolds on multipotent mesenchymal stromal cells. *Appl Biochem Biotechnol* 2008; 49: 185–194.
225. Freeman JW, Woods MD, Cromer DA, et al. Tissue engineering of the anterior cruciate ligament: the viscoelastic behavior and cell viability of a novel Braid-twist scaffold. *J Biomater Sci-Polym Ed* 2009; 20: 1709–1728.
226. Hofvendahl K and Hahn-Hägerdal B. Factors affecting the fermentative lactic acid production from renewable resources(1). *Enzyme Microb Technol* 2000; 26: 87–107.
227. Auras R, Harte B and Selke S. An overview of polylactides as packaging materials. *Macromol Biosci* 2004; 4: 835–864.
228. Zhou S, Shanmugam KT, Yomano LP, et al. Fermentation of 12% (w/v) glucose to 1.2 M lactate by *Escherichia coli* strain SZ194 using mineral salts medium. *Biotechnol Lett* 2006; 28: 663–670.
229. Datta R and Henry M. Lactic acid: recent advances in products, processes and technologies—a review. *J Chem Technol Biotechnol* 2006; 81: 1119–1129.
230. González MI, Álvarez S, Riera F, et al. Economic evaluation of an integrated process for lactic acid production from ultrafiltered whey. *J Food Eng* 2007; 80: 553–561.
231. Adsul MG, Varma AJ and Gokhale DV. Lactic acid production from waste sugarcane bagasse derived cellulose. *Green Chem* 2007; 9: 58–62.
232. Singhvi M, Joshi D, Adsul M, et al. D(–)-lactic acid production from cellobiose and cellulose by *Lactobacillus lactis* mutant RM2-24. *Green Chem* 2010; 12: 1106–1109.
233. Abdel-Rahman MA, Tashiro Y and Sonomoto K. Lactic acid production from lignocellulose-derived sugars using lactic acid bacteria: overview and limits. *Biotechnol J* 2011; 156: 286–301.
234. Ulery BD, Nair LS and Laurencin CT. Biomedical applications of biodegradable polymers. *J Polym Sci B-Polym Phys* 2011; 49: 832–864.
235. Uzun N, Martins TD, Teixeira GM, et al. Poly(L-lactic acid) membranes: absence of genotoxic hazard and potential for drug delivery. *Toxicol Lett* 2015; 232: 513–518.
236. Lovald ST, Khraishi T, Wagner J, et al. Mechanical design optimization of bioabsorbable fixation devices for bone fractures. *J Craniofac Surg* 2009; 20: 389–398.
237. Chen Y, Mak AFT, Wang M, et al. PLLA scaffolds with biomimetic apatite coating and biomimetic apatite/collagen composite coating to enhance osteoblast-like cells attachment and activity. *Surf Coat Technol* 2006; 201: 575–580.
238. Philp A, Macdonald AL and Watt PW. Lactate—a signal coordinating cell and systemic function. *J Exp Biol* 2005; 208: 4561–4575.
239. Uehlin AF, Vines JB, Feldman DS, et al. Uni-directionally oriented fibro-porous PLLA/Fibrin bio-hybrid Scaffold: mechano-morphological and cell studies. *Pharmaceutics* 2022; 14: eng1015340031999.
240. Li X, Cheng R, Sun Z, et al. Flexible bipolar nanofibrous membranes for improving gradient microstructure in tendon-to-bone healing. *Acta Biomater* 2017; 61: 204–216.

241. Sajkiewicz P, Heljak MK, Gradys A, et al. Degradation and related changes in supermolecular structure of poly (caprolactone) in vivo conditions. *Polym Degrad Stab* 2018; 157: 70–79.
242. Song C, Wang P, Sun H, et al. The in vivo degradation, adsorption and excretion of poly(epsilon-caprolactone). *J Biomed Eng* 2000; 17: 25–28.
243. Cao Y, Yang S, Zhao D, et al. Three-dimensional printed multiphase scaffolds with stratified cell-laden gelatin methacrylate hydrogels for biomimetic tendon-to-bone interface engineering. *J Orthop Translat* 2020; 23: 89–100.
244. Smith LL, Niziolek PJ, Haberstroh KM, et al. Decreased fibroblast and increased osteoblast adhesion on nanostructured naoh-etched PLGA scaffolds. *Int J Nanomedicine* 2007; 2: 383–388.
245. Erisken C, Kalyon DM and Wang H. Functionally graded electrospun polycaprolactone and beta-tricalcium phosphate nanocomposites for tissue engineering applications. *Biomaterials* 2008; 29: 4065–4073.
246. Erisken C, Kalyon DM, Wang H, et al. Osteochondral tissue formation through adipose-derived stromal cell differentiation on biomimetic polycaprolactone nanofibrous scaffolds with graded insulin and beta-glycerophosphate concentrations. *Tissue Eng Part A* 2011; 17: 1239–1252.
247. Tabata Y. The importance of drug delivery systems in tissue engineering. *Pharm Sci Technol Today* 2000; 3: 80–89.
248. Pina S, Ribeiro VP, Marques CF, et al. Scaffolding strategies for tissue engineering and regenerative medicine applications. *Materials* 2019; 12: eng1015559291996.
249. Cooper JO, Bumgardner JD, Cole JA, et al. Co-cultured tissue-specific scaffolds for tendon/bone interface engineering. *J Tissue Eng* 2014; 5: 2041731414542294.
250. Shen W, Chen J, Yin Z, et al. Allogeneous tendon stem/progenitor cells in silk scaffold for functional shoulder repair. *Cell Transplant* 2012; 21: 943–958.
251. McGoldrick R, Chattopadhyay A, Crowe C, et al. The tissue-engineered tendon-bone interface: in vitro and in vivo synergistic effects of adipose-derived stem cells, platelet-rich plasma, and extracellular matrix hydrogel. *Plast Reconstr Surg* 2017; 140: 1169–1184.
252. Zhao H, Chen W, Chen J, et al. ADSCs promote tenocyte proliferation by reducing the methylation level of lncRNA morf411 in tendon injury. *Front Chem* 2022; 10: 908312.
253. Nourissat G, Diop A, Maurel N, et al. Mesenchymal stem cell therapy regenerates the native bone-tendon junction after surgical repair in a degenerative rat model. *PLoS One* 2010; 5: e12248.
254. Lim J, Hui J, Li L, et al. Enhancement of tendon graft osteointegration using mesenchymal stem cells in a rabbit model of anterior cruciate ligament reconstruction. *Arthrosc- J Arthrosc Relat Surg* 2004; 20: 899–910.
255. Hashimoto Y, Yoshida G, Toyoda H, et al. Generation of tendon-to-bone interface “Enthesis” with use of recombinant BMP-2 in a rabbit model. *J Orthop Res* 2007; 25: 1415–1424.
256. Yonemitsu R, Tokunaga T, Shukunami C, et al. Fibroblast growth factor 2 enhances tendon-to-bone healing in a rat rotator cuff repair of chronic tears. *Am J Sports Med* 2019; 47: 1701–1712.
257. Kovacevic D, Fox AJ, Bedi A, et al. Calcium-phosphate matrix with or without TGF- $\beta$ 3 improves tendon-bone healing after rotator cuff repair. *Am J Sports Med* 2011; 39: 811–819.
258. Holladay C, Abbah SA, O’Dowd C, et al. Preferential tendon stem cell response to growth factor supplementation. *J Regen Med Tissue Eng* 2016; 10: 783–798.
259. Cheng X, Tsao C, Sylvia VL, et al. Platelet-derived growth-factor-releasing aligned collagen-nanoparticle fibers promote the proliferation and tenogenic differentiation of adipose-derived stem cells. *Acta Biomater* 2014; 10: 1360–1369.
260. Cheng P, Han P, Zhao C, et al. High-purity magnesium interference screws promote fibrocartilaginous entheses regeneration in the anterior cruciate ligament reconstruction rabbit model via accumulation of BMP-2 and VEGF. *Biomaterials* 2016; 81: 14–26.
261. Kim YI, Ryu JS, Yeo JE, et al. Overexpression of TGF- $\beta$ 1 enhances chondrogenic differentiation and proliferation of human synovium-derived stem cells. *Biochem Biophys Res Commun* 2014; 450: 1593–1599.
262. Durant TJ, Dymont N, McCarthy MB, et al. Mesenchymal stem cell response to growth factor treatment and low oxygen tension in 3-dimensional construct environment. *Muscles Ligaments Tendons J* 2014; 4: 46–51.
263. Cicione C, Muiños-López E, Hermida-Gómez T, et al. Alternative protocols to induce chondrogenic differentiation: transforming growth factor- $\beta$  superfamily. *Cell Tissue Bank* 2015; 16: 195–207.
264. Kataoka T, Mifune Y, Inui A, et al. Combined therapy of platelet-rich plasma and basic fibroblast growth factor using gelatin-hydrogel sheet for rotator cuff healing in rat models. *J Orthop Surg Res* 2021; 16: 605.
265. Chen J, Liao L, Lan T, et al. Treated dentin matrix-based scaffolds carrying TGF- $\beta$ 1/BMP4 for functional bio-root regeneration. *Appl Mater Today* 2020; 20: 1–16. DOI: 10.1016/j.apmt.2020.100742
266. Font Tellado S, Chiera S, Bonani W, et al. Heparin functionalization increases retention of TGF- $\beta$ 2 and GDF5 on biphasic silk fibroin scaffolds for tendon/ligament-to-bone tissue engineering. *Acta Biomater* 2018; 72: 150–166.
267. Kingma JJ, de Knikker R, Wittink HM, et al. Eccentric overload training in patients with chronic Achilles tendinopathy: a systematic review. *Br J Sports Med* 2007; 41: e3.
268. Chiquet M, Gelman L, Lutz R, et al. From mechanotransduction to extracellular matrix gene expression in fibroblasts. *Biochim Biophys Acta Mol Cell Res* 2009; 1793: 911–920.
269. Buxboim A, Ivanovska IL and Discher DE. Matrix elasticity, cytoskeletal forces and physics of the nucleus: how deeply do cells ‘feel’ outside and in? *J Cell Sci* 2010; 123: 297–308.
270. Riehl BD, Park JH, Kwon IK, et al. Mechanical stretching for tissue engineering: Two-Dimensional and three-dimensional constructs. *Tissue Eng Part A* 2012; 18: 288–300.
271. Govoni M, Berardi AC, Muscari C, et al. An engineered multiphase three-dimensional microenvironment to ensure

- the controlled delivery of cyclic strain and human growth differentiation factor 5 for the tenogenic commitment of human bone marrow mesenchymal stem cells. *Tissue Eng Part A* 2017; 23: 811–822.
272. Wang T, Chen P, Zheng M, et al. In vitro loading models for tendon mechanobiology. *J Orthop Res* 2018; 36: 566–575.
273. Wang T, Lin Z, Day RE, et al. Programmable mechanical stimulation influences tendon homeostasis in a bioreactor system. *Biotechnol Bioeng* 2013; 110: 1495–1507.
274. Wang T, Lin Z, Ni M, et al. Cyclic mechanical stimulation rescues achilles tendon from degeneration in a bioreactor system. *J Orthop Res* 2015; 33: 1888–1896.
275. Altman GH, Horan RL, Martin I, et al. Cell differentiation by mechanical stress. *FASEB J* 2002; 16: 270–272.
276. Rinoldi C, Costantini M, Kijeńska-Gawrońska E, et al. Tendon tissue engineering: Effects of mechanical and biochemical stimulation on stem cell alignment on cell-laden hydrogel yarns. *Adv Healthc Mater* 2019; 8: e1801218.
277. Tucker JJ, Cirone JM, Morris TR, et al. Pulsed electromagnetic field therapy improves tendon-to-bone healing in a rat rotator cuff repair model. *J Orthop Res* 2017; 35: 902–909.
278. Huegel J, Chan PYW, Weiss SN, et al. Pulsed electromagnetic field therapy alters early healing in a rat model of rotator cuff injury and repair: Potential mechanisms. *J Orthop Res* 2022; 40: 1593–1603.